Version 1.0

Update to Proposal P-909:
Physics Performance of the CDF II Detector with
An Inner Silicon Layer
and
A Time of Flight Detector

The CDF Collaboration

Submitted to the Fermilab Director and PAC

5 January 1999

1 Introduction

On 22 September 1998, the CDF Collaboration submitted a proposal (P-909) to the Fermilab director and Program Advisory Committee (PAC) entitled: "*Proposal for Enhancement of the CDF II Detector: An Inner Silicon Layer and a Time of Flight Detector.*" This proposal was presented to the PAC on 23 October 1998. We proposed two additions to the CDF II baseline detector:

1. **Layer-00:** This additional inner layer of silicon would be mounted on the beampipe at a radial distance of 1.6cm from the beam. This additional layer would serve two primary purposes: first, as it would sit inside our silicon tracker SVX II, it would enhance our impact parameter resolution and improve significantly our ability to tag b quark jets. The impact parameter resolution of a track with transverse momentum $p_T = 1$ GeV/c would improve to $\sim 25\mu$m compared to $\sim 50\mu$m with SVX II alone. Second, it is made out of a new type of silicon that can be operated at much higher bias voltages. The detector can continue to operate, therefore, after significant radiation damage, and serves as a prototype for a silicon tracker for the intense luminosity (10^{33}cm^{-2}s^{-1}) expected in Run III of the Tevatron.

2. **Time-of-Flight (TOF):** This detector would be installed at a radius of 138cm from the beam in the 6cm of radial space between the main drift-chamber (the Central Outer Tracker or COT) and the cryostat of the superconducting solenoid. It would be used to measure the time-of-flight of charged particles from the $p\bar{p}$ interaction point with a precision of 100psec. This detector would significantly increase our particle identification capabilities: in particular, it would allow separation of kaons and pions with a statistical precision of two standard deviations up to a momentum of 1.6 GeV/c. This would enhance our b flavor tagging, which is a crucial component of precise measurements of neutral B meson flavor oscillations and CP asymmetries in the decays of B mesons. It would double our flavor tagging effectiveness for B_s^0 mesons. As Fermilab is considering a dedicated B physics experiment in Run III, the TOF would also provide crucial data (instead of Monte Carlo data) to study the effectiveness of kaon identification in the environment of a hadron collider.

Several physics studies were presented in the proposal to illustrate the utility of these additional detectors. These studies included the increased b quark jet tagging efficiency for the reconstruction of t quark decays, the increased b flavor tagging efficiency in the measurement of CP asymmetries in neutral B meson decays such as $B^0/\bar{B}^0 \to J/\psi K^0_{\mathrm{S}}$, and increased b flavor tagging efficiency and proper decay time resolution in the measurement of B_s^0 meson decays, in particular, the precise measurement of B_s^0 flavor oscillations. Since B_s^0 mesons are not produced on the $\Upsilon(4S)$, this physics will be unique to hadron colliders[1],

[1] The one current exception is the SLD experiment operating on the Z^0 resonance at the SLC at SLAC.

and dominated by the Tevatron during the first half of the next decade. The precise measurement of B_s^0 flavor oscillations is particularly important because it is a crucial part of testing unitarity of the Cabibbo-Kobayashi-Maskawa matrix when combined with already existing precise measurements of B_d^0 flavor oscillations. The proposal described a study of B_s^0 flavor oscillations that predicted that CDF could see these oscillations if the B_s^0 mixing parameter is in the range $x_s < 42$. This alone covers the currently favored value within the Standard Model [1]. With the addition of Layer 00 and TOF, this reach is extended to $x_s < 63$. Given the importance of this measurement and the unique sensitivity reported by CDF, the PAC focused its questions on our predicted reach for B_s^0 flavor oscillations. The PAC posed several questions, which are listed below, to the collaboration. This Report contains the response to these questions.

1.1 Questions from the PAC

In response to our proposal, the director communicated the following questions to us in a letter dated 11 November 1998. The full text of this letter can be found in Appendix A. The questions concerning our sensitivity to B_s^0 flavor oscillations are paraphrased below:

1. The collaboration should report on what trigger was assumed for the mixing studies, how its efficiency was estimated, and the reliability of these estimates in the face of real-life conditions such as noise and multiple interactions per crossing.

2. The collaboration should justify their use of the DELPHI signal to background given the very different B momentum spectrum and event environments at the Tevatron and LEP.

3. The collaboration should provide studies of the benefits of the TOF for suppressing background, including $B_s^0 \to D_s^- \pi^+$ and $B_s^0 \to D_s^- \pi^+ \pi^- \pi^+$ mass plots.

4. In all studies, the collaboration should specify the luminosity assumed and should provide the results for the baseline detector and for the detector upgraded with L00 and the TOF separately and together.

5. The committee would like the results of these studies in January.

6. In addition, the committee recommends that the collaboration begin to develop a detailed Monte Carlo simulation of B decays, as this tool will be essential as CDF pursues B physics.

2 Overview of Measuring B_s^0 Flavor Oscillations

The measurement of B_s^0 flavor oscillations requires a proper decay time dependent measurement. This requires

1. Reconstruction of the proper decay time of the B_s^0. The addition of Layer 00 provides an important improvement here.

2. Determining the flavor of the B_s^0 at production, *i.e.*, did it contain a b or a $\bar{b}$ quark. TOF plays a crucial role here.

3. Determining the flavor of the B_s^0 at decay. For the decay modes considered in this Report, the final state identifies the flavor at decay unambiguously.

The signature for flavor oscillations is

$$\frac{N_{\text{unmixed}}(t) - N_{\text{mix}}(t)}{N_{\text{unmixed}}(t) + N_{\text{mix}}(t)} = D \cdot \cos\left(\frac{x_s}{\tau(B_s^0)}t\right), \tag{1}$$

where $N_{\text{unmixed}}(t)$ ($N_{\text{mix}}(t)$) are the number of decays at proper decay time t in which the flavor at production is the same (opposite) the flavor at decay, x_s is the mixing parameter, which is related to the mass difference between the two mass eigenstates by $x_s = \Delta m_s \tau(B_s^0)$, and D is the dilution of the flavor tag, which is related to the probability $\mathcal{P}$ that the flavor tag at production is correct: $D = 2\mathcal{P} - 1$. The proper decay time t is not measured with infinite precision, and this introduces further dampening of the amplitude of the cosine. Of course measuring the flavor oscillations is predicated on the ability to extract a B_s^0 signal with adequate statistics and signal-to-noise.

In Run I, the CDF collaboration proved it could reconstruct B_s^0 mesons with excellent signal-to-noise. We were limited by our trigger, however, to reconstructing either semileptonic decays such as $B_s^0 \to D_s^- \ell^+ \nu_\ell X$ ($\ell = e$ or μ), or fully reconstructed decays involving $J/\psi \to \mu^+\mu^-$ decays, *e.g.*, $B_s^0 \to J/\psi\phi$. Precise measurements of the B_s^0 lifetime were published [2] based on these signals, and the semileptonic decays were used to make the first direct limit on the difference in width $\Delta\Gamma_s$ between the two B_s^0 mass eigenstates. The signals are shown in Figures 1 and 2. We also have a preliminary result on the CP composition of $B_s^0 \to J/\psi\phi$ using a transversity analysis.

This fully reconstructed state is a CP eigenstate and cannot be used to measure B_s^0 flavor oscillations, but we can use semileptonic decays. The proper time t is determined from the measured decay length L and the momentum p:

$$t = m(B) \cdot \frac{L}{p}, \tag{2}$$

where $m(B)$ is the mass of the B hadron. The uncertainty δt on t is

$$(\delta t)^2 = \left(\frac{m(B)}{p}\delta L\right)^2 \oplus \left(t \cdot \frac{\delta p}{p}\right)^2, \tag{3}$$

where δL and δp are the uncertainties on the decay length and momentum, respectively. The semileptonic decays are only partially reconstructed. This means not all of the B momentum is measured, and this degrades the proper time resolution at larger t according to the second term in equation 3. Nevertheless, there is some sensitivity to B_s^0 flavor oscillations in our current data set. We searched for B_s^0 flavor oscillations in a dilepton triggered data sample. One lepton was associated to a ϕ and an additional hadron to form a partially reconstructed sample of semileptonic B decays with a B_s^0 purity of 60%. The second lepton in the event was used to tag the flavor of the B_s^0 at production. No evidence for B_s^0 flavor oscillations was seen, and a lower limit of $\Delta m_s > 5.8\ \text{ps}^{-1}$ at 95% C.L. was established. This result [3] has been submitted to Physical Review Letters.

To increase our reach in Run II, we need fully reconstructed decays such as $B_s^0 \to D_s^- \pi^+$. This requires a trigger to collect hadronic decays without a J/ψ in the final state, that is, an all-hadronic B decay trigger. The Silicon Vertex Trigger or SVT, a new component of the CDF trigger system for Run II that will be used to exploit the long lifetime of B hadrons, was motivated by this need. The SVT makes it possible to identify tracks with significant impact parameters at the second level of the trigger. The initial development of an all-hadronic B trigger using the SVT focused on collecting a large sample of two-body hadronic B decays such as $B^0 \to \pi^+\pi^-$. We have expanded the two-body hadronic B decay trigger to include modes such as $B_s^0 \to D_s^- \pi^+$, with $D_s^- \to \phi\pi^-$. In all our studies presented here, we assume that SVT will perform as designed. We did not have this hardware in Run I, so this is new territory for us. Nevertheless, our existing data includes test runs as well as standard triggers that have been used for the studies presented in this Report. The SVT uses only axial information from SVX II, and the geometry of SVX II is similar to the geometry of the Run IB silicon detector SVX$'$. We have used, therefore, data from SVX$'$ and passed these data through a simulation of the SVT to estimate the all-hadronic B trigger rate. This reduces the dependence on Monte Carlo imposed on all other experiments at hadron colliders proposing to trigger on all-hadronic B decays. These studies of the all-hadronic B trigger and the estimates for signal rates for B_s^0 are presented in Section 3.

Even if we are able to collect large samples of hadronic B decays with our trigger, there is still the question of whether or not we can extract the signals with acceptable signal-to-noise. The combinatorial background originates from two distinct sources:

1. heavy flavor production, namely $b\bar{b}$ and $c\bar{c}$ production, and

2. light-quark and gluon production (QCD jets).

This second source has a production cross-section that is between two orders and three orders of magnitude larger than $b\bar{b}$ production; however, the impact parameter requirements in the second level of the trigger reduce this background significantly. In the limit of perfect impact parameter resolution, we would expect combinatorial background only from events with displaced decays, namely heavy flavor production. Our minimum bias data samples are too small to search for hadronic B decays or to even study the combinatorial background.

We must use, therefore, our inclusive lepton data samples (electron and muon), which are enriched in heavy flavor production. These samples are collected with an inclusive lepton trigger, which requires a lepton with $p_T > 8$ GeV/c approximately. These data are from semileptonic b and c decay, and QCD background in which a hadron causes a fake signal of a lepton in the detector. For the events in which the lepton originates from B hadron decay, we can attempt to reconstruct the other B hadron in an all-hadronic decay mode. We start by first reconstructing charm signals opposite the lepton, and then we try combining the observed charm signals with one (*i.e.*, $D\pi$) and three (*i.e.*, $D\pi\pi\pi$) charged tracks to search for a B signal. These studies are presented in Section 4 and are very much "work-in-progress." Despite their preliminary nature, they indicate that it is plausible that the combinatorial background from heavy flavor production is manageable, and they have the advantage, again, of being based on data, instead of Monte Carlo. We can also use these data to study the combinatorics from QCD background: in the inclusive electron sample, we can identify electrons originating from photon conversions. These conversions are dominated by QCD background.

Following the presentation of our trigger performance, expected signal rates, and anticipated signal-to-noise, we present our expected sensitivity to $B_s^0 - \bar{B}_s^0$ flavor oscillations in Section 5. These expectations are based on the same studies presented in our original proposal, but are repeated here to form a self-contained documentation of this work.

Finally, in Section 6 we discuss current studies and studies planned in the near future.

3 Hadronic B Trigger and Expected Signal Rates

In Run I, the CDF trigger had three levels. The first two levels were implemented in hardware. The first level triggered on objects such as clusters in the electromagnetic calorimeter (*e.g.*, electrons and photons), or track-segments in the muon chambers. The second level included track reconstruction in the Central Fast Track (CFT) processor [4], and the capability to perform limited event reconstruction (*e.g.*, match a CFT track to an electromagetic cluster to form an electron candidate). The third level was a farm of Silicon Graphics computers in which the data were processed and filtered using a version of the offline data reconstruction program that was optimized for execution speed.

In Run II, the trigger will continue to have three levels, but the through-put of each level will be increased by more than an order of magnitude from the Run I trigger to accommodate the shorter $p\bar{p}$ crossing interval (initially 396ns, and eventually 132ns), and the order of magnitude increase in instantaneous luminosity. The maximum output of Level 1 will be 50KHz and the maximum output of Level 2 will be 300Hz. The CFT has been replaced by the eXtremely Fast Tracker (XFT), which has significantly better p_T resolution and is implemented at Level 1, instead of Level 2. Data from the silicon tracker (SVX II) will be available at Level 2. The Silicon Vertex Trigger (SVT) can associate clusters in SVX II with XFT tracks, providing enough precision that the lifetime of heavy flavors may be exploited to trigger on B hadron decays at Level 2. The third level will consist of a farm of PCs running LINUX. A description of the Run II trigger, including the XFT and SVT, can be found in the CDF II *Technical Design Report* [5].

The feasibility of a trigger for hadronic B decays without final-state leptons in CDF has been studied since the 1993 Snowmass Workshop on B Physics at Hadron Accelerators [6]. At that time, work focussed on triggering on $B^0 \to \pi^+\pi^-$ decays. This work led to the development of the Two-Track Level 1 trigger and the SVT for Level 2. Because Δm_s is now known to be large [7], its measurement will require fully reconstructed B_s decays in order to achieve the necessary momentum resolution, as discussed previously in Section 2. Therefore, we expanded the studies to include selections for hadronic decays of B_s. Although this Report focuses on B_s mixing, we include information on $B^0 \to \pi^+\pi^-$ as well since the trigger selections have large overlap, and the sensitivity to a *CP*-violating asymmetry in $B^0 \to \pi^+\pi^-$ is important as well.

The B_s decays modes of greatest experimental interest have only charged particles in the final state and relatively low multiplicity. The modes used in this study are $B_s^0 \to D_s^-\pi^+$and $B_s^0 \to D_s^-\pi^+\pi^-\pi^+$. The assumed branching fractions are listed in Table 1. We have also included $B_s^0 \to D_s^{*-}\pi^+$, which may also be useful since the photon in the D_s^* decay carries little momentum so that the B_s^0 mass and momentum resolution are not seriously degraded. Our estimates for our sensitivity to x_s do not include this mode, however. We have studied trigger rates for these modes using minimum bias data[2] for Level 1 and data sets collected with specialized test triggers taken in Run IB for Level 2. The signal yields are estimated using a parametric Monte Carlo simulation that accounts for the geometry of the SVX II. The Monte Carlo generates single b quarks according to the p_T and rapidity y spectrum of Nason, Dawson, and Ellis [9]. Correlated production of $b\bar{b}$ pairs is generated according to the calculation of Mangano, Nason, and Ridolfi [10]. The b quarks are fragmented into B hadrons using the Peterson [11] function with the fragmentation parameter value $\epsilon_b = 0.006$. The B hadrons are decayed using the CLEO Monte Carlo program `QQ` [12]. The cross sections and branching fractions used to estimate the yields are listed in Table 1. Because the B_s branching fractions are not measured, we use measured B^0 branching fractions for analogous decay modes. The measurement of the B_s production fraction f_s in $p\bar{p}$ collisions from CDF [13] is larger (but less precise) than those from LEP. Although the fragmentation fractions from $p\bar{p}$ and e^+e^- production may not be identical, to be conservative, we use the LEP values. The cross section is normalized to the CDF measurement [8]. There is a correlated uncertainty of 40% on the signal yields due to the uncertainties in the production cross section $\sigma(B^0)$, the production fraction of B_s^0 mesons f_s, and the branching fraction $\mathrm{Br}(D_s^- \to \phi\pi^-)$. When the uncertainties on the B_s^0 branching fractions are included, the total uncertainties on the signal yields vary from 40% to 50%, depending on the particular channel. These uncertainties greatly exceed any statistical uncertainties in our Monte Carlo

[2]These data are triggered by a forward-backward coincidence of beam-beam scintillator counters (BBC) and are intended to be an unbiased sample of inelastic $p\bar{p}$ collisions.

Quantity	Value	Source
$\mathrm{Br}(B^0 \to \pi^+\pi^-)$	1.0×10^{-5}	Assumption
$\mathrm{Br}(B_s^0 \to D_s^-\pi^+)$	$0.30 \pm 0.04\%$	Analogous B^0 channel [7]
$\mathrm{Br}(B_s^0 \to D_s^{*-}\pi^+)$	$0.28 \pm 0.02\%$	Analogous B^0 channel [7]
$\mathrm{Br}(B_s^0 \to D_s^-\pi^+\pi^-\pi^+)$	$0.80 \pm 0.25\%$	Analogous B^0 channel [7]
$\mathrm{Br}(D_s^- \to \phi\pi^-)$	$3.6 \pm 0.9\%$	[7]
$\mathrm{Br}(D_s^- \to K^{*0}K^-)$	$3.3 \pm 0.9\%$	[7]
f_s/f_d	0.26 ± 0.05	LEP average [7]
$\sigma(p\bar{p} \to B^0X)$ $(p_T(B^0) > 6$ GeV$/c$, $\lvert y\rvert < 1)$	$2.39 \pm 0.54\,\mu$b	CDF measurement [8]

Table 1: The branching fractions, the production of B_s^0 relative to B^0 (f_s/f_d), and the B^0 production cross section used in this Report.

studies. In our estimates of our sensitivity to x_s, we have varied the estimates of our signal yields by 50%.

We describe the Level 1 trigger selection and rates in Section 3.1, the Level 2 selection and rates in Section 3.2, and the predicted yields in Section 3.3.

3.1 Two-Track Level 1 Trigger

The original motivation of this trigger was the selection of a large sample of two-body B decays, in particular, $B^0 \to \pi^+\pi^-$. The inclusive p_T spectrum of charged particles in $p\bar{p}$ collisions at $\sqrt{s} = 1.8$ TeV falls rapidly with p_T approximately as p_T^{-8} [14]. The charged particle p_T spectrum from B hadron decay produced by the hard-scattering process $p\bar{p} \to b\bar{b}X$ is significantly harder. The selection of two-tracks above a p_T threshold is the initial step in reducing the background of inelastic collisions relative to B hadron production. Furthermore, tracks from B decay are correlated in angle, and often the two tracks with the largest p_T from B decay have opposite charge, so we exclude track pairs that are back-to-back in azimuth and require that the two tracks have opposite charge.

The Level 1 selection uses tracks found by the XFT track processor. The XFT can find tracks of $p_T > 1.5\,\mathrm{GeV}/c$ that traverse the full radius of the COT with a momentum resolution $\delta p_T/p_T^2 < 0.015\,(\mathrm{GeV}/c)^{-1}$ and an azimuthal resolution at superlayer 6 (R=106 cm) of $\delta\phi_6 < 0.0015$ rad. All tracks with p_T exceeding a selectable threshold $p_{T\mathrm{min}}$ are fed to the two-track trigger module. The two-track module compares the values of p_T and ϕ_6 from all pairs of tracks to valid trigger patterns in a lookup table. In order to limit the number of combinations that must be evaluated, events with seven or more tracks exceeding the threshold are automatically accepted.

Three sets of two-track trigger criteria are listed in Table 2. In addition to the individual track p_T threshold $p_{T\mathrm{min}}$ and the restriction on maximum separation in azimuth $\delta\phi_{6,\mathrm{max}}$, there is a minimum requirement $(\Sigma p_T)_{\rm min}$ on the scalar sum $\Sigma p_T = p_{T,1} + p_{T,2}$ of the transverse momenta of the two tracks. Scenarios A, B, and C correspond to three possible operating conditions of the Tevatron. The scenarios cover the possible bunch separations ($T_{\rm bunch}$), instantaneous luminosity ($\mathcal{L}$), and mean number of interactions per crossing ($\langle N_{p\bar{p}}\rangle$).

Scenario	$T_{\rm bunch}$ (ns)	$\mathcal{L}$ ($\times 10^{32}{\rm cm}^{-2}{\rm s}^{-1}$)	$\langle N_{p\bar{p}}\rangle$	$p_{T{\rm min}}$ (GeV/c)	$(\Sigma p_T)_{\rm min}$ (GeV/c)	$\delta\phi_{6,{\rm max}}$
A	396	0.7	2	2.00	5.5	135°
B	132	2.0	2	2.25	6.0	135°
C	396	1.7	5	2.50	6.5	135°

Table 2: Level 1 trigger criteria for the three operating scenarios studied.

Figures 3 and 4 show the distributions of p_T and Σp_T respectively, for CDF minimum bias events and those expected for the $B_s^0 \to D_s^- \pi^+$ and $B^0 \to \pi^+\pi^-$ channels. Figures 5 and 6 show the efficiency for the p_T and Σp_T requirements, respectively, as a function of the minimum requirement. In all four Figures, we require $\delta\phi_6 < 135^\circ$ to suppress back-to-back combinations. These Figures illustrate that the p_T spectrum of the background is significantly softer, and falls more rapidly, than the signal. If the trigger rates are unexpectedly high, we can always increase $p_{T{\rm min}}$ and $(\Sigma p_T)_{\rm min}$ to reduce the rates, without unacceptable loss of signal.

The Level 1 two-track trigger rate will be dominated by QCD background in which the two tracks that satisfy the trigger requirement each come from

- a single $p\bar{p}$ interaction, or
- a *different* $p\bar{p}$ interaction, during bunch crossings with multiple $p\bar{p}$ interactions.

To determine the trigger rates, we must simulate the pattern of hits generated in the COT and then feed these hits to the XFT simulation. We can not use directly the CTC data, since the COT has approximately five times as many sense wires as the CTC, and a different geometry. We must use, therefore, the COT simulation to generate hits from tracks. We must be sure, however, to use a distribution of tracks that will have the correct angular and kinematic correlations between charged particles from the same interaction, as well as from different interactions in the same bunch crossing. At the same time we must be sure that we produce the correct hit multiplicity. We have accomplished this by combining a sample of minimum bias events from Run IB with events produced by the CDF minimum bias Monte Carlo, MBR, to generate a sample of simulated Run II events with the various interaction multiplicities. The Run IB sample of minimum bias events was collected at low luminosity so that each event contains only one interaction per crossing. The CTC reconstruction was greater than 98% efficient for charged particles with $p_T > 0.5\,{\rm GeV}/c$, and pseudorapidity

$|\eta| < 1$. We can use, therefore, the minimum-bias data to generate hits from tracks with $p_T > 0.5\,\mathrm{GeV}/c$, and pseudorapidity $|\eta| < 1$. We still need, however, to generate hits from charged particles at larger η or with smaller p_T. These hits are generated using tracks from the MBR Monte Carlo. We have found the number of MBR events necessary per minimum bias data event such that the combination reproduces the CTC hit occupancy observed in the Run IB data. We use this same number to generate hits in the COT.

The number of interactions per event is varied according to Poisson statistics, and the positions of the interaction vertices are distributed according to the expected longitudinal beam profile. The generated events are processed with the same detector simulation that was used in preparation of the *Technical Design Report* [5] to create a list of COT wire hits. This list provides the input to a full simulation of the XFT. The resulting trigger rates for each of the scenarios are given in Table 3. The Level 1 bandwidth is 50 kHz, and we expect to allocate a maximum of 30 kHz to the two-track trigger: all three operating scenarios are predicted to be at or below this maximum rate. Again, if the trigger rates are unexpectedly high, we can always adjust the Level 1 selection criteria to reduce the rates, without unacceptable loss of signal.

We also studied the XFT fake rate in these samples. We define a fake as an XFT track that on the basis of the measured resolutions is inconsistent in curvature or ϕ_6 with all tracks used to generate the simulated data. The fake rate is less than 4%. The XFT efficiency is expected to exceed 97% per track.

Scenario	Two-track cross section (μb)	Two-track rate (kHz)
A	252 ± 18	18
B	152 ± 14	30
C	163 ± 16	28

Table 3: Level 1 trigger rates for three operating scenarios outlined in Table 2.

3.2 Level 2

At Level 2, we use the SVT, which associates clusters formed from axial strips in the SVX II with tracks of $p_T > 2\,\mathrm{GeV}/c$ found in the COT by the XFT. This provides an improved measurement of p_T and the azimuthal direction at the beamline ϕ_0. More important, it also provides a measurement of the closest distance of approach to the beam line (or “impact parameter”) of the track in the plane transverse to the beam axis. The measurement of the impact parameter is sufficiently precise so that we can resolve the true large impact parameters of tracks coming from the decays of heavy flavor from the impact parameters of tracks coming from QCD jets, which have non-zero impact parameter only due to measurement resolution. The SVT sends a list of tracks to the Level 2 Alpha processors. The first step of our Level 2 selection is to find pairs of tracks with significant impact parameters that also satisfy the Level 1 requirements. Next we find the intersection point of these two tracks, and we require that the vector pointing from the beam line to this point, $\vec{X}_v$, satisfy $\vec{p}_T \cdot \vec{X}_v > 0$, where $\vec{p}_T = \vec{p}_{T,1} + \vec{p}_{T,2}$. Two random mismeasured tracks from QCD background that intersect will have $\vec{p}_T \cdot \vec{X}_v > 0$ and $\vec{p}_T \cdot \vec{X}_v < 0$ with equal probability, but two tracks originating from the decay of a B hadron predominately have $\vec{p}_T \cdot \vec{X}_v > 0$. We have studied selections both for hadronic B_s decays and for $B^0 \to \pi^+\pi^-$. In the latter case, all decay products of the B are found so we can require that the impact parameter of the two-track combination d_B is consistent with zero, *i.e.*, the B candidate points back to the beam line. This allows the $B^0 \to \pi^+\pi^-$ selection to have a looser requirement on the track impact parameter d_0. We optimize the opening angle requirement separately for the two selections. In both cases we exclude large impact parameters to suppress fakes and photon conversions as well as K_S and Λ daughters. Although the two kaons resulting from $D_s^- \to \phi\pi^-$ decays have a small opening angle, we nevertheless exclude small-angle track pairs from our trigger. In the SVT simulations described below, we found that excluding small-angle track pairs reduced the expected trigger rate by nearly 50%. We attribute this to a high fake rate in dense hit environments. Because the pions in $B_s^0 \to D_s^-\pi^+$, $D_s^- \to \phi\pi^-$ events tend to be higher momentum than the kaons, requiring $\Delta\phi_0 > 2°$ has less than 10% inefficiency for this mode. Our Level 2 selection requirements are summarized in Table 4.

B_s hadronic	$B^0 \to \pi^+\pi^-$
$120\ \mu\text{m} < \lvert d_0 \rvert < 1$ mm	$100\ \mu\text{m} < \lvert d_0 \rvert < 1$ mm
$2° < \Delta\phi_0 < 90°$	$20° < \Delta\phi_0 < 135°$
$p_T \cdot X_v > 0$	$p_T \cdot X_v > 0$
—	$d_B < 140\,\mu\text{m}$

Table 4: Level 2 trigger selection requirements

In order to derive accurate estimates of the trigger rates, it is necessary to use a detailed SVT simulation with event samples that include the correct detector occupancies. Therefore, we again use the Run IB data and simulate the performance of the SVT using track patterns optimized for the geometry of the Run IB silicon detector, SVX′. Since only 1 out of every 200 minimum bias events passes the planned Level 1 trigger selection, it is not possible to get a large enough minimum bias sample for Level 2 studies. Therefore, we use data collected in several test runs that had a two-track requirement using the CFT track processor. The sample contains about 400,000 events from two Tevatron stores and corresponds to an integrated luminosity of approximately 1 μb^{-1}. This is an order of magnitude more integrated luminosity than the entire CDF Run I minimum bias data sample.

Because the XFT efficiency is high and the XFT fake rate is low, it is not necessary to perform a full simulation of the XFT on this sample. We use tracks found by the standard CDF offline reconstruction smeared by the XFT resolutions. The geometry of the inner four layers of SVX II is quite similar to that of the SVX′. Therefore, rate estimates based on SVX′ data should be accurate when corrected for the increased longitudinal acceptance of SVX II. We derive a set of track patterns for the SVX′ geometry using the same procedures that will be used to derive patterns for the SVX II. To be conservative, we use all channels of SVX′ without noisy-channel suppression, while in reality this may be carried out in the SVT hardware.[3] The baseline plan for the SVT is to require hits in each of the inner four layers of the SVX II. Therefore, it is quite natural to simulate this requirement in the SVX′. Because the gaps between SVX II barrels lead to substantial inefficiency, we believe that we can improve SVT efficiency by requiring hits in 4 out of 5 SVX II layers. This would also help maintain trigger efficiency if the innermost layer of SVX II starts to lose efficiency due to radiation damage. But we do not believe we can make accurate predictions of trigger rates with a 4/5 requirement until we have Run II data.

We find the numbers of event that satisfy the requirements for each of the three Level 1 scenarios and that satisfy either the B_s or $B^0 \to \pi^+\pi^-$ Level 2 requirements of Table 4. The trigger cross section is found by

$$\sigma = f_z \frac{N}{\mathcal{L}}, \tag{4}$$

where N is the number of events passing the trigger requirements, $\mathcal{L}$ is the integrated luminosity of the test data, and f_z is a factor to account for the increased longitudinal acceptance of the SVX II. To account for the increased z length of the SVX II detector, we define $\epsilon(z_0)$ to be the geometric acceptance for a track to intersect the inner four layers as a function of the track origin z_0. We do this for both SVX′ and SVX II detector geometries and calculate a correction factor by convoluting $\epsilon(z_0)$ with the distribution $g(z_0)$ of primary event vertices.

$$f = \frac{\int g(z_0)\epsilon_{II}^2(z_0)dz_0}{\int g(z_0)\epsilon_I^2(z_0)dz_0} = 2.5. \tag{5}$$

The expected trigger rates for the B_s and $B^0 \to \pi^+\pi^-$ selections are given in Table 5. The two trigger selections have a large overlap, so we also present the combined rate. The expected rates are well below the total Level 2 bandwidth for all triggers of 300 Hz. Several factors, not yet taken into account, may increase the trigger rate. In the SVX II, the hybrids containing the readout chips overlap the active detector region. This overlap leads to approximately twice as much material compared to SVX′ over about one third of the length of SVX II. We have estimated the effect of the additional material by degrading the impact parameter resolution of simulated tracks that pass through this extra material. This increases

[3] In our simulations of SVT in the Run 1B data, noisy-channel suppression reduced predicted trigger rates by about 30%. However, we cannot know the effect on the signal rate until the noisy-channel rate in the SVX II is known. Therefore, we do not allow for any noise suppression in our rate estimates.

Scenario	B_s selection		$B^0 \to \pi^+\pi^-$ selection		Both selections		Level 2 Rate (Hz)
A	394	± 105	360	± 100	560	± 125	39
B	280	± 89	196	± 74	336	± 97	67
C	196	± 74	84	± 48	224	± 79	38

Table 5: Level 2 trigger cross sections in nanobarns for the three Level 1 scenarios. The errors are the statistical errors based on the number of events passing the selection criteria in the data.

the trigger rate by 10%. This does not account for any effects on the pattern recognition, or for hard scatters. Studies to understand these effects are in progress. In addition, we have not superimposed events to simulate higher luminosity conditions. The data from the two stores have luminosities equivalent to Run II conditions of $\mathcal{L} = 0.3 \times 10^{32}\mathrm{cm}^{-2}\mathrm{s}^{-1}$ and $\mathcal{L} = 0.9 \times 10^{32}\mathrm{cm}^{-2}\mathrm{s}^{-1}$ at 396 ns crossing period. Using a looser set of requirements, we observe no dependence of the trigger cross section on the instantaneous luminosity within the limited statistical precision available in our samples. If multiple interactions do present a problem, we can mitigate the increased rate from random combinations by requiring the two tracks to have their innermost hit in the same 14 cm half-barrel of the SVX II. Just as with the Level 1 rates, if the Level 2 rates are unexpectedly high, we can always adjust the Level 2 selection criteria (*e.g.*, the impact parameter requirement, see Figure 7 and the discussion in the following Section) to reduce the rates without unacceptable loss of signal.

3.3 Signal yield

To estimate the signal yield, we generate $B_s^0 \to D_s^{(*)-}\pi^+(\pi^-\pi^+)$ and $B^0 \to \pi^+\pi^-$ using the Monte Carlo described earlier in this Section. The B production point is selected randomly according to the expected 25 μm R.M.S. transverse beam envelope and the 28 cm R.M.S. longitudinal beam profile. The B_s^0 and D_s^- decay positions are generated using their measured lifetimes. The geometry of the SVX II is approximated as a set of five concentric cylinders with radii equal to the mean radii of the ladders. We track the paths of final state particles through the cylinders to determine whether they cross within the fiducial range along the z coordinate. We account for all expected gaps in z between sensors in this way. On the basis of experience with SVX$'$, we assign a 98% efficiency for making a hit if a track is within the fiducial acceptance of a layer of silicon. For a track to be considered usable by the trigger, it must be simulated to have hits in the inner 4 SVX$'$ layers and must traverse all COT axial superlayers. A track is considered fiducial if it is simulated to have hits in any 3 out of the 5 SVX II layers and exits the COT at a radius greater than 110 cm, consistent traversing at least 3 axial superlayers. For each trigger-usable track, we apply a 90% efficiency for satisfy-

Mode	A	B	C
$B_s^0 \to D_s^- \pi^+$	5.3pb	4.2pb	3.6pb
$B_s^0 \to D_s^- \pi^+ \pi^- \pi^+$	6.4pb	5.2pb	4.1pb
$B_s^0 \to D_s^{*-} \pi^+$	4.7pb	3.7pb	2.9pb
$B^0 \to \pi^+ \pi^-$	7.6pb	5.9pb	4.2pb

Table 6: Cross section in picobarns for B decay modes of interest where all final-state charged hadrons are observed in the CDF tracking fiducial.

ing an SVT pattern in the associative memory and smear the impact parameter according to a resolution function determined in a full hit-level Monte Carlo simulation. The resolution used in this study is

- $\delta d_0 = [19 + (40\,\mathrm{GeV}/c)/p_T]\mu$m for tracks that miss the hybrid in Layer 0;
- $\delta d_0 = [19 + (80\,\mathrm{GeV}/c)/p_T]\mu$m for tracks that pass through the hybrid in Layer 0.

An event is considered available for analysis if all final-state daughter tracks are fiducial and there is a pair of tracks that are found by SVT and satisfy all Level 1 and Level 2 requirements. The cross sections for analyzable events for decay modes of interest for the three operating scenarios are given in Table 6. Figure 7 shows the expected trigger cross section for the B_s selections and the cross section for analyzable $B_s^0 \to D_s^- \pi^+$ events as a function of the selection requirement on impact parameter.

For our estimates of our sensitivity to B_s^0 flavor oscillations, we assume we will collect 2fb^{-1} of data in two years. The corresponding numbers of signal events are listed in Table 7. As mentioned earlier, the uncertainties on these numbers ranges from 40% to 50%, and are highly correlated. In our estimates, we combine the expected number of events for $B_s^0 \to D_s^- \pi^+$ and $B_s^0 \to D_s^- \pi^+ \pi^- \pi^+$ to obtain a total number of signal events. This total varies from 23400 if all the data were taken using Level 1 scenario A to 15300 if all the data is taken using Level 1 scenario C. We vary this total by from 5000 to 30000 when we evaluate our x_s reach.

4 Signal-to-Noise in B Hadronic Final States

As summarized in Table 7 of Section 3, we expect to collect large samples of $B_s^0 \to D_s^- \pi^+$ and $B_s^0 \to D_s^- \pi^+ \pi^- \pi^+$. The next question we must address is whether or not we will be able to extract these signals from the potentially enormous combinatorial background. The combinatorial background originates from two distinct sources:

1. heavy flavor production, namely $b\bar{b}$ and $c\bar{c}$ production, and

Mode	A	B	C
$B_s^0 \to D_s^- \pi^+$	10600	8400	7200
$B_s^0 \to D_s^- \pi^+ \pi^- \pi^+$	12800	10400	8100
$B_s^0 \to D_s^{*-} \pi^+$	9400	7400	5800
$B^0 \to \pi^+ \pi^-$	15200	11800	8400

Table 7: Sample sizes expected in 2fb^{-1} of data for the B decay modes of interest corresponding to the cross sections reported in Table 6.

2. light-quark and gluon production (QCD background).

Charged particles from b hadron and c hadron decay can satisfy both the kinematic requirements and the impact parameter requirements of the trigger. We expect the kinematic requirements and the smaller mass and shorter lifetimes of charm particles to suppress the c background relative to the b background. The background from $b\bar{b}$ can be modeled reliably, but this involves generating a large sample of $b\bar{b}$ Monte Carlo events. Our measured cross section of $\sigma(p\bar{p} \to B^0 X, p_T(B^0) > 6\ \text{GeV}/c, |y(B^0)| < 1) = 2.39 \pm 0.54\ \mu\text{b}$, corresponds to approximately 10^{10} $b\bar{b}$ events in 2 fb^{-1}. We are working on a scheme to generate such a Monte Carlo sample efficiently, but we were unable to do so for this Report. Instead we have used our Run I data samples, as described later in this Section.

The QCD background has a production cross-section that is between two-orders and three-orders of magnitude larger than $b\bar{b}$ production, even after the kinematic requirements of the Level 1 trigger have been applied. However, the impact parameter requirements in the second level of the trigger reduce this background significantly. The impact parameter requirements can be satisfied by this background only when the trajectories of charged particles are badly mismeasured, or when tracks originate from photon conversions or hadronic interactions in the detector material, or from the decay of strange particles. Although in principle it is possible to model these affects, in practice it is impractical, so again, we must rely on our current data to estimate this background.

We can get an initial indication of the importance of the combinatorial background from QCD compared to the background from inclusive B production from an estimate of the fraction of the trigger sample that comes from $b\bar{b}$ production. This estimate is based on generator-level[4] Monte Carlo combined with the CLEO `QQ` B decay simulation [12]. We use three Monte Carlos of $b\bar{b}$ production: `PYTHIA` [15], `HERWIG` [16], and a generator based on a next-to-leading order QCD calculation [10]. The p_T spectra and azimuthal correlations of the b and $\bar{b}$ are quite similar for all three generators, and the predicted trigger rates due to $b\bar{b}$ production are equal within $\pm 5\%$. To estimate the effect of the impact parameter

[4] This means we produce the four vectors of the decay products of B hadrons, but we do not apply a detailed simulation of the Run II detector to these events.

requirements in Level 2, we use a parameterization of the nominal SVX II resolution. To determine the trigger rates due to $b\bar{b}$, we count the number of events passing the Level 1 and Level 2 trigger requirements. These rates are normalized to our measured cross section [8] (2.39μb for B^0 production with $p_T(B^0) > 6$ GeV/c and $|y| < 1$).

For trigger scenario A, we obtain the following average rates from the three Monte Carlo generators: $\sigma_{b\bar{b}}$(Level 1) = (720 ± 20) nb, and $\sigma_{b\bar{b}}$(Level 2) = (81 ± 4) nb. These yields may be compared with the rates measured in the real data: (252 ± 18) μb for Level 1 and (394 ± 105) nb for Level 2 (B_s^0 selection only). As expected, the $b\bar{b}$ contribution to the Level 1 cross sections is small, of order 0.3% of the measured Level 1 rate. However, with the SVT impact parameter cuts in Level 2, the predicted fraction of triggers coming from $b\bar{b}$ production improves substantially, to around 24% of the total measured Level 2 yield for the B_s^0 Level 2 selection.

This indicates that the expected $b\bar{b}$ purity after Level 2 is very high, typical of the purity we currently obtain with J/ψ (20%) and inclusive lepton triggers (40%). We have reconstructed $B \to J/\psi K$ and $\bar{B} \to \ell^- \bar{\nu} D X$ decays in these samples successfully with excellent signal-to-noise. Therefore, we expect that the $b\bar{b}$ combinatorial backgrounds will dominate the combinatorial backgrounds from the QCD background in the all-hadronic trigger modes as well.

To study the combinatorial background from $b\bar{b}$ production, we have attempted to reconstruct a hadronic B signal in our inclusive lepton data sets. The trigger requires either an electron or a muon with $p_T > 8$ GeV/c. Approximately 40% of these events come from semileptonic decay of B hadrons. Since B hadrons are produced in pairs, these events contain a second B hadron with a decay that is not biased by the trigger. In approximately 40% of these events, this second B hadron is within the fiducial acceptance of the CTC (*i.e.*, $|\eta| < 1$). We attempt to reconstruct D mesons opposite the lepton, and then combine the reconstructed D mesons with one or three charged tracks with the appropriate charge correlations to look for B candidates. The D mesons we reconstruct are (charge conjugate modes are implied)

- $D^0 \to K^- \pi^+$;
- $D^{*+} \to D^0 \pi^+$, D^0 reconstructed as above;
- $D^+ \to K^- \pi^+ \pi^+$;
- $D_s^+ \to \phi \pi^+$, with $\phi \to K^+ K^-$;

Significant signals are seen in all four channels. The signals are shown in Figure 8. The D^+ signal is of particular interest, since it is topologically similar to the D_s^+ signal (a three-prong vertex, although the D^+ lifetime is significantly longer), and has much higher statistics. The selection criteria used to extract these signals are less restrictive than the criteria that will be imposed by the displaced two-track trigger. The D^+ signal that is observed after applying the Level 1 and Level 2 trigger criteria specified in Section 3 to the events is shown in Figure 9.

Applying these stricter criteria improves the signal to background from approximately 1:6 to 1:4. The next step is to combine these D signals with either a single track, which is assumed to be a pion, or a combination of three tracks. The tracks are selected to have the expected charge correlation, *e.g.*, π^- or $\pi^-\pi^-\pi^+$ with D^+. The resulting mass plots in the case of the D^+ are shown in Figure 10. In order to interpret these distributions in term of signal-to-background, we need an estimate of the expected signal. Preliminary estimates indicate that the expected signal is comparable to the background found in these plots, *i.e.*, assuming a signal to background in the range of 1:2 to 2:1 is reasonable. This is work in progress, and we will continue to refine this analysis to obtain more quantitative estimates of the background due to $b\bar{b}$.

5 Sensitivity to B_s^0-$\bar{B}_s^0$ Oscillations

The most powerful tool for observing of B_s^0-$\bar{B}_s^0$ oscillations is the ability to trigger on B_s^0 decays which can be fully reconstructed. It is also necessary to tag their production flavor in order to classify them as being mixed or unmixed at the time when they decayed. A measurement of the B_s^0-$\bar{B}_s^0$ mixing frequency, $\Delta m_s = x_s/\tau$, can be made by fitting the mixed asymmetry,

$$A_{\text{mixed}}(t) = \frac{N_{\text{unmixed}}(t) - N_{\text{mixed}}(t)}{N_{\text{unmixed}}(t) + N_{\text{mixed}}(t)} \tag{6}$$

to a function of the form

$$a(t) = A \cos x_s t/\tau. \tag{7}$$

If the fit is performed by minimizing a log-likelihood quantity, the significance of a measurement of x_s can be defined in terms of the depth of the minimum. The significance can be expressed in "equivalent standard deviations" by

$$\text{Sig} = \sqrt{2\Delta \log \mathcal{L}} \tag{8}$$

where $\Delta \log \mathcal{L}$ is the depth of the minimum compared to the next-to-deepest minimum, or in general, to the value of $\log \mathcal{L}$ as $x_s \to \infty$.

This significance can be expressed analytically by the formula

$$\text{Sig}(x_s) = \sqrt{\frac{N\epsilon D^2}{2}} e^{-(x_s \sigma_{ct}/\tau)^2/2} \sqrt{\frac{S}{1+S}} \tag{9}$$

where N is the number of B_s^0 decays reconstructed (untagged), ϵ and D are the tagging efficiency and dilution, respectively, σ_{ct} is the resolution with which the proper decay time is reconstructed and S is the signal-to-background ratio of the B_s^0 sample; $\tau = 1.54$ ps[7] is the B_s^0 lifetime. Figure 11a shows a comparison of this formula with the average significance obtained from *ensembles* of Monte Carlo experiments. Figure 11b compares the shape of the

$-\log\mathcal{L}$ curves from various simulated experiments with the shape expected from a similar analytic expression. There is generally good agreement between the analytic expressions and results obtained by averaging ensembles of Monte Carlo experiments. Therefore, we use the formula given in equation 9 to estimate the maximum value of x_s for which a significant observation of B_s^0-$\bar{B}_s^0$ oscillations could be made under various assumptions for the parameters N, ϵD^2, σ_{ct} and S. This use of this formula allows one to scale our projections for different values of the assumed input parameters.

We consider four possible detector upgrade scenarios: the CDF baseline configuration, the addition of TOF and Layer 00 separately, and the addition of both TOF and Layer 00 combined. TOF doubles the tagging efficiency by providing opposite-side and same-side kaon tags. We use (see Section 5.3 in P-909)

$$\epsilon D^2 = \begin{cases} 5.7\% & \text{without TOF} \\ 11.3\% & \text{with TOF} \end{cases} \tag{10}$$

for the effective tagging efficiencies. The significance of an observation scales with $\sqrt{\epsilon D^2}$ for any value of x_s. The addition of Layer 00 will provide more precise decay length measurements which will improve the proper time resolution. We use (see P-909)

$$\sigma_{ct} = \begin{cases} 60 \text{ fs} & \text{without Layer 00} \\ 45 \text{ fs} & \text{with Layer 00} \end{cases} \tag{11}$$

in the following discussion of the sensitivity to B_s^0-$\bar{B}_s^0$ oscillations. The range of x_s for which oscillations would be observed at a given level of significance is inversely proportional to the proper time resolution.

Figure 12 shows the significance of observations of B_s^0-$\bar{B}_s^0$ mixing as a function of x_s for the four upgrade scenarios and for signal-to-background ratios of 2:1 and 1:2. The curves shown in this figure assume $N = 20,000$ as well as values for the other parameters given by equations 10 and 11. This figure illustrates the separate benefits provided by TOF and Layer 00 in different regions of x_s. In the range $x_s < 32$, where the oscillation period is large compared with the proper time resolution provided by SVX II alone, the addition of TOF would enhance the significance of an observation by roughly a factor of $\sqrt{2}$. This will be particularly important if we fall short of our goal of $N(B_s^0) = 20,000$ or if backgrounds are higher than expected. TOF will also be used to improve the signal-to-background ratio in the $\bar{B}_s^0$ sample which will increase the significance of any observation of oscillations, regardless of the frequency. If $x_s > 32$ then the range for which a significant observation of B_s^0-$\bar{B}_s^0$ oscillations could be made is more effectively extended by the addition of Layer 00.

Table 8 shows the maximum value of x_s for which an observation of mixing would be made with a significance of at least 5σ for various values of $N(B_s^0)$ and for signal-to-background ratios of 1:2 and 2:1. This range of $N(B_s^0)$ is expected to encompass all trigger scenarios described in Section 3. The signal-to-background ratios in the range from 1:2 to 2:1 is reasonable based on the preliminary studies described in Section 4.

$N(B_s^0)$	S/B=2:1				S/B=1:2			
	Baseline	TOF	L00	TOF+L00	Baseline	TOF	L00	TOF+L00
5,000	30	36	40	49	21	30	27	39
10,000	37	42	49	56	30	36	40	49
20,000	42	47	56	63	37	42	49	56
30,000	45	50	61	67	40	45	53	60

Table 8: Maximum values of x_s for which observation of mixing could be made with at least 5σ significance. Values for signal-to-background ratios of 2:1 and of 1:2 are shown.

$N(B_s^0)$	$x_s = 30$				$x_s = 40$			
	Baseline	TOF	L00	TOF+L00	Baseline	TOF	L00	TOF+L00
5,000	2.20	0.53	0.61	0.24	—	—	2.20	0.53
10,000	0.52	0.21	0.23	0.11	—	1.01	0.52	0.21
20,000	0.21	0.10	0.10	0.05	0.99	0.34	0.21	0.10
30,000	0.13	0.06	0.07	0.03	0.50	0.20	0.13	0.06

Table 9: Minimum values of the signal-to-background ratio for which observation of mixing could be made with at least 5σ significance. The dashes indicate scenarios for which a 5σ observation could not be made even in the absence of any background.

Table 9 shows the how low the signal-to-background ratio can be before a 5σ observation of B_s^0-$\bar{B}_s^0$ oscillations can no longer be made, for $x_s = 30$ and $x_s = 40$. This table illustrates how signal purity must be favorable, if we are to observe B_s^0-$\bar{B}_s^0$ oscillations with a B_s^0 sample smaller than anticipated with the baseline detector. The demand on signal purity is relaxed significantly with the addition of TOF and Layer 00.

To conclude, if x_s is in the range expected by the Standard Model and current experimental constraints[1], we should observe B_s^0-$\bar{B}_s^0$ oscillations in Run II even for rather pessimistic scenarios for the B_s^0 sample size and signal-to-background. In some scenarios, the observation of B_s^0-$\bar{B}_s^0$ oscillations is possible only with the addition of TOF and Layer 00. while in others they will provide an important increase in significance. In addition, they will also extend the x_s range for which a significant observation could be made, well beyond the values currently expected and into regions anticipated for new physics scenarios.

Once oscillations are observed, their frequency will be measured extremely precisely. These additional upgrades provide important insurance that the great investment already made in SVX II and the secondary vertex trigger will indeed result in the precise measurement of the B_s^0-$\bar{B}_s^0$ mixing frequency. This measurement is not an end in itself, but instead it would represent the beginning of a new program of physics. Since CP asymmetries are modulated by the oscillation frequency, the search for, and the study of, CP violating effects in the B_s^0 system will benefit greatly from the enhancements provided by TOF and Layer 00.

6 Plans for Future Studies

The studies presented in this Report are at various levels of maturity. Some of the studies are based on work that has been in progress for several years (*e.g.*, the trigger rate studies), while others are only a few months old. We will continue these studies until we begin collecting Run II data. We hope that we will make substantial progress in the near future on further quantifying our expected background in the all-hadronic B decay modes. We are beginning an effort to generate a large $b\bar{b}$ Monte Carlo sample with a detailed simulation of the Run II detector, in particular of the Run II tracking system. This should allow us to investigate, for example, non-Gaussian tails in the reconstructed B_s^0 lifetime, and may also help us with understanding how often tracks from primary particles (*e.g.*, fragmentation particles from b quark hadronization) are misreconstructed and appear to have significant impact parameter.

We have not addressed the question concerning how particle identification from TOF could help improve the signal to background in the reconstruction of B hadrons. Again, this is a study we have begun and will continue in the next months. We can get some indication of the potential using our current Run I data. In Run I, our only particle identification was based on dE/dx from the outer six layers of the CTC. The dE/dx resolution was approximately 10%, and provided π-K separation that was typically on the order of one standard deviation, or slightly better, in the region of the relativistic rise. Despite this limited particle separation, the dE/dx played an important role in many of our published papers. We illustrate this with two examples. The first is the use of dE/dx to identify protons in the reconstruction of the decay $\Lambda_c^+ \to pK^-\pi^+$. The Λ_c^+ was combined with a lepton to provide a clean signature of the decay of the Λ_b^0 baryon, $\Lambda_b^0 \to \ell^-\bar{\nu}_\ell\Lambda_c^+X$. Using this signal, CDF published a measurement of the Λ_b^0 lifetime [17]. Figure 13 shows the reconstructed $\Lambda_c^+ \to pK^-\pi^+$ both before (upper curve) and after (lower curve) identification of the proton with dE/dx has been required. The proton identification reduced the combinatorial background substantially with an acceptable loss of efficiency for the signal. TOF provides a separation of two standard deviations of protons from pions up to a momentum of 3.2 GeV/c.

The second example is the rejection of combinatorial background in the partial reconstruction of B_s^0 decays used in a search for B_s^0-$\bar{B}_s^0$ flavor oscillations [3]. The signature was $B_s^0 \to \ell^-\bar{\nu}_\ell\phi X$, with $\phi \to K^+K^-$. The dE/dx was used to reduce the combinatorial background in the ϕ, as illustrated in Figure 14. The kaons in this plot have $p_T(K) > 1.0$ GeV/c, well within the range that TOF would provide powerful K-π separation. Again, despite the narrow width of the ϕ, particle identification is very important in reducing combinatorial background.

7 Conclusions

We repeat here the PAC questions and summarize our responses.

1. The collaboration should report on what trigger was assumed for the mixing studies, how its efficiency was estimated, and the reliability of these estimates in the face of real-life conditions such as noise and multiple interactions per crossing.

   The trigger is an all-hadronic B Decay trigger that uses tracks at Level 1 and impact parameter at Level 2. We have estimated the rate of this trigger using data collected during Run I of the Tevatron, which takes into account noise and multiple interactions. These are the most reliable estimates we can make, until we get Run II data. The signal yields are estimated using Monte Carlo with the B hadron production cross-section normalized to the CDF measurement. We include a $\pm 50\%$ *uncertainty on the signal rates in the estimates of our reach for* x_s.

2. The collaboration should justify their use of the DELPHI signal to background given the very different B momentum spectrum and event environments at the Tevatron and LEP.

   We are no longer relying on results from the LEP experiments to justify our expected signal to background. Instead, we have looked at our own Run I data. This study is still in progress, but preliminary indications indicate that our assumed range of signal to background of 1:2 to 2:1 is reasonable. The committee has been provided with enough information to determine our reach for x_s *for a more pessimistic value of signal to background, as well. Results on signal to background from Run I data are a pessimistic estimate of the signal to background since the Run I silicon detector only provides two-dimensional measurements in the plane transverse to the beamline, but SVX II will provide a three-dimensional space point. This could have a significant impact, particularly for two-body modes such as* $B^0 \to \pi^+\pi^-$.

3. The collaboration should provide studies of the benefits of the TOF for suppressing background, including $B_s^0 \to D_s^-\pi^+$ and $B_s^0 \to D_s^-\pi^+\pi^-\pi^+$ mass plots.

   We have begun these studies, but have not reported on them here. We illustrated the potential with two examples of using dE/dx *in our Run I data. TOF provides significantly better separation that* dE/dx *in a part of the momentum range important for reconstructed B hadrons, so we believe it will have an impact.*

4. In all studies, the collaboration should specify the luminosity assumed and should provide the results for the baseline detector and for the detector upgraded with L00 and the TOF separately and together.

   The studies presented here are for $2fb^{-1}$ *of data. The sensitivity to* B_s^0 *flavor oscillations has been presented separately for all four configurations: (1) baseline detector,* *(2) baseline with TOF, (3) baseline with Layer 00, and (4) baseline with TOF and Layer 00.*

5. The committee would like the results of these studies in January.

   We tried to provide as much new information as possible.

6. In addition, the committee recommends that the collaboration begin to develop a detailed Monte Carlo simulation of B decays, as this tool will be essential as CDF pursues B physics.

   We agree with this recommendation and we are working on the most efficient means to generate a large sample of inclusive B hadron decays with a detailed simulation of the Run II detector that can be used, in particular, to study details of the tracking performance.

We hope that this supplement to proposal P-909 will help the PAC arrive at the conclusion that both TOF and Layer 00 are powerful additions to the CDF detector, particularly in the study of B physics. The precise measurement of B_s^0 flavor oscillations is a cornerstone of the test of unitarity of the CKM Matrix that is unique to hadron colliders and SLD in the near future. We have demonstrated that TOF and Layer 00 are complementary detectors for the measurement of x_s. The TOF system makes the most significant improvement at lower x_s (< 30). The Layer 00 upgrade is more important at high x_s (> 40). Although we have presented plausible arguments based on our best knowledge that we expect high yields in the number of B_s^0 events, lower yields are quite possible. Both these upgrades are more powerful if the event yield is low (5000 events).

Observing B_s^0 flavor oscillations would be the beginning of a plethora of important measurements in the B_s^0 system, including measurements of CP asymmetries in B_s^0 decays. The impact of TOF on b flavor tagging and the improvement from Layer 00 on proper decay time resolution could be even more important for these measurements.

The studies presented in this report should help convince the PAC that CDF has designed a practical trigger to collect very large samples of hadronic B decays, allowing us to take advantage of the enormous B production cross section at the Tevatron. All other experiments devoted to the study of B physics have realized that particle identification is crucial and have made major investments in detectors that will provide excellent particle identification capabilities. CDF will need particle identification as well to extract the most physics from our large samples of B hadron decays. Time-of-flight is the most economical and the only practical means for us to augment our particle identification capabilities for Run II.

We emphasize that both TOF and Layer 00 have many more applications that we have not explored in the detailed studies presented in this Report. Better vertex resolution and event-by-event particle identification are crucial for extending the physics reach of an already very powerful baseline CDF-II detector.

References

[1] see, for example, F. Parodi, P. Roudeau, and A. Stocchi, *Constraints on the parameters of the $V_{\rm CKM}$ matrix at the end of 1997*, LAL-98-49, Feb. 1998, hep-ph/9802289.

[2] The CDF Collaboration, F. Abe *et al.*, Phys. Rev. Lett. **74**, 4988 (1995).
The CDF Collaboration, F. Abe *et al.*, Phys. Rev. Lett. **77**, 1945 (1996).
The CDF Collaboration, F. Abe *et al.*, Phys. Rev. D **57**, 5382 (1998).
The CDF Collaboration, F. Abe *et al.*, *Measurement of the B_s^0 Lifetime using Semileptonic Decays*, FERMILAB–PUB–98/172–E, accepted for publication in Phys. Rev. D.

[3] The CDF Collaboration, F. Abe *et al.*, *A Search for $B_s^0 - \bar{B}_s^0$ Oscillations Using the Semileptonic Decay $B_s^0 \to \phi\ell^+X\nu$*, FERMILAB–PUB–98/401–E, submitted to Phys. Rev. Lett.

[4] G. W. Foster *et al.*, Nucl. Instrum. Methods A **269**, 93 (1988).

[5] The CDF II Collaboration, R. Blair *et al.*, *The CDFII Detector Technical Design Report*, Fermilab-PUB-96/390-E. This Report may be found at the following world-wide web URL: http://www-cdf.fnal.gov/upgrades/tdr/tdr.html.

[6] J. D. Lewis, J. Mueller, J. Spalding, and P. Wilson, *Proceedings of the Workshop on B Physics at Hadron Accelerators*, Snowmass, Colorado, 21 June - 2 July 1993, Fermilab-CONF-93/267, pp. 217-20;
G. Punzi, S. Donati, and G. Gagliardi, *op. cit.*, pp. 227-8.

[7] C. Caso *et al.*, *Review of Particle Properties*, *European Physics Journal C,* **3,** 1 (1998).

[8] The CDF Collaboration, F. Abe *et al.*, Phys. Rev. Lett., **75**, 1451 (1995).

[9] P. Nason, S. Dawson, and R. K. Ellis, Nucl. Phys. **B327**, 49 (1989).

[10] M. Mangano, P. Nason, and G. Ridolfi, Nucl. Phys. **B373**, 295 (1992).

[11] C. Peterson *et al.*, Phys. Rev. D **27**, 105 (1983).

[12] P. Avery, K. Read, and G. Trahern, Cornell Internal Note CSN-22, 1985 (unpublished).

[13] The CDF Collaboration, F. Abe *et al.*, Phys. Rev. D **54**, 6596 (1996).

[14] The CDF Collaboration, F. Abe *et al.*, Phys. Rev. Lett. **61**, 1819 (1988).

[15] H. U. Bengtsson and T. Sjöstrand, Computer Physics Commun. **43**, 43 (1987);
T. Sjöstrand, Computer Physics Commun. **82**, 74 (1994).

[16] G. Marchesini and B. R. Webber, Nucl. Phys. **B136**, 1 (1978).

[17] The CDF Collaboration, F. Abe *et al.*, Phys. Rev. Lett. **77**, 1945 (1996).

A Letter from Fermilab Director

Thank you for the presentation at the recent PAC meeting on the new proposal for the addition of a L00 silicon layer and TOF device to CDF (P-909). The PAC's comments follow:

P-909 - CDF (Bedeschi/Goshaw)

CDF proposes a new silicon layer (L00) mounted on the beam pipe. Addition of the layer would improve impact parameter resolution by more than 30 percent, would preserve vertexing capabilities should L0 succumb to radiation damage, and would be the first trial of the rad-hard technology that CDF is considering for a replacement silicon detector in the later part of Run II. One important beneficiary of the improved tracking is CDF's sensitivity to B_s mixing. For their conservative assumptions about backgrounds, use of L00 would extend CDF's reach in x_s from about 35 to 47 and improve its resolution at x_s = 30 from 15 percent to 11 percent. No other experiment with comparable reach in x_s is likely to run in the same time period.

The Committee finds the L00 upgrade very attractive and encourages the Laboratory and the collaboration to pursue it strongly. The Committee notes that the collaboration has found most of the funding for this project.

CDF also proposes installation of a TOF device outside the COT. By providing 2 sigma K-pi separation over the range 0.4<p<1.6 GeV, this detector would improve flavor tagging for B_d and B_s and might reduce combinatorial background to B decays. For B_s decays, epsilon D^2 would double, extending the reach in x_s to 54 and improving the x_s resolution at x_s = 30 to 8 percent.

The Committee believes that the TOF would be a useful addition to CDF. The collaboration has considered installing only the scintillator before the start of Run II, postponing installation of the PMT's and electronics. This appears to be a sensible approach if full funding has not been obtained by the start of Run II.

The Committee would like further information regarding CDF's sensitivity to B_s mixing. Areas of particular importance are the trigger and backgrounds. Regarding the trigger, the collaboration should report on what trigger was assumed for the mixing studies, how its efficiency was estimated, and the reliability of these estimates in the face of real-life conditions such as noise and multiple interactions per crossing. Regarding the backgrounds, the collaboration should justify their use of the DELPHI signal to background given the very different B momentum spectrum and event environments at the Tevatron and LEP. It should also provide studies of the benefits of the TOF for suppressing background, including B_s -> D_s pi and B_s -> D_s pi pi pi mass plots. In all studies, the collaboration should specify the luminosity assumed and should provide the results for the basline detector and for the detector upgraded with L00 and the TOF separately and together. The Committee would like the results of these studies in January. In addition, the Committee recommends that the collaboration begin to develop a detailed Monte Carlo simulation of B decays, as this tool will be essential as CDF pursues B physics.

The Committee notes that the Laboratory's funds for new projects are very limited and the availability of unused contingency is very unlikely, and urges the collaboration to seek outside funds.

Please plan on making a presentation to the PAC on the studies on trigger and backgrounds as noted above at the January 15-17 meeting. You should also present a detailed plan on how these upgrades are to be funded. Written documentation should be submitted no later than Tuesday, January 5 so that it may be sent to the PAC before the meeting.

Sincerely,

John Peoples

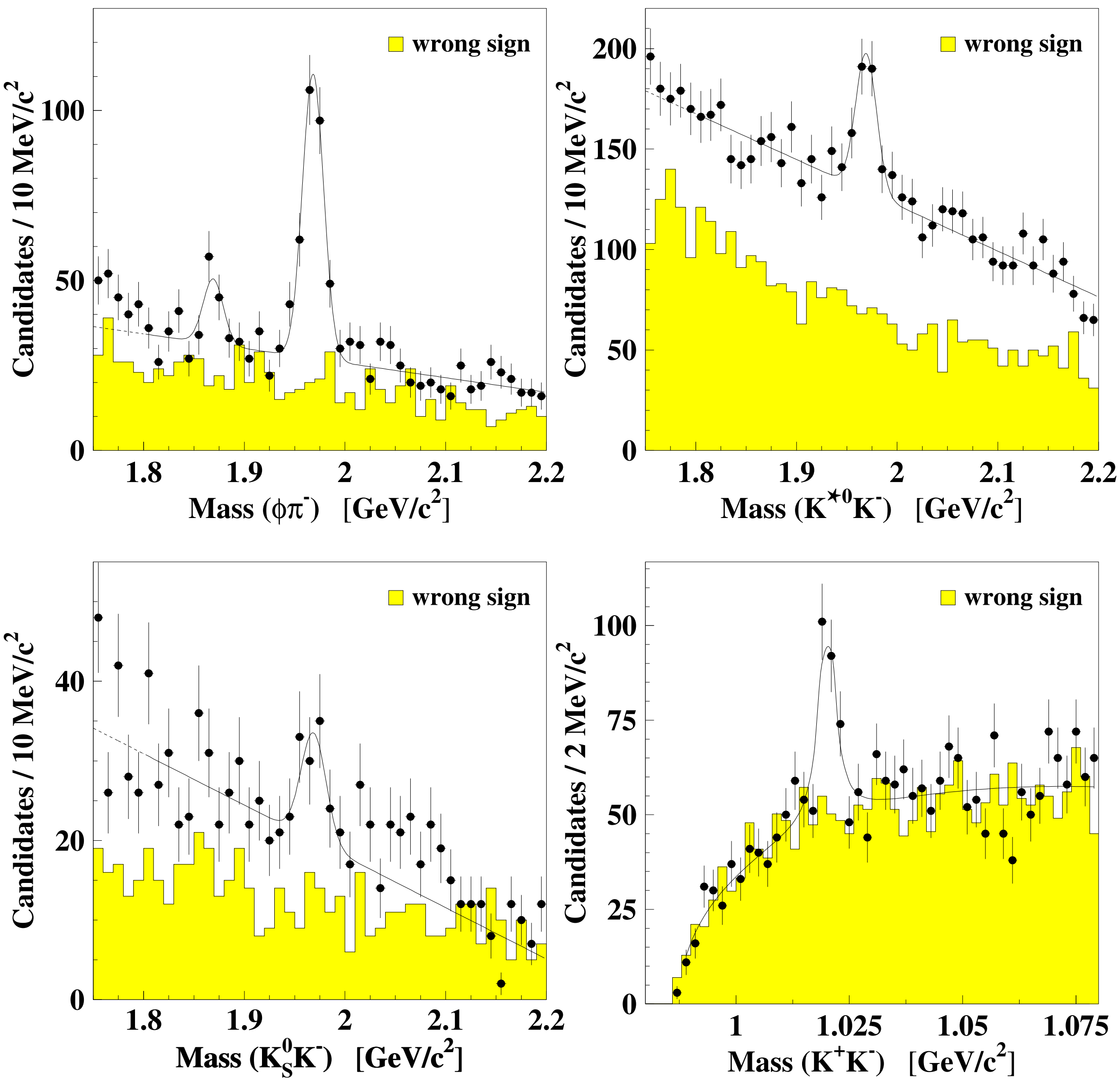

Figure 1: The mass spectra of the D_s^- mesons reconstructed in four different decay modes: (a) upper-left: $D_s^- \to \phi\pi^-$, (b) upper-right: $D_s^- \to K^{*0}K^-$, (c) lower-left: $D_s^- \to K_S^0 K^-$, and (d) lower-right: $D_s^- \to \phi\ell^-\bar{\nu}X$. These D_s^- mesons are associated with a lepton (ℓ) and are presumed to originate from the semileptonic decay of a $\bar{B}_s^0$ (The charge conjugate modes are included as well). The points with error bars are the data for the case that the D_s and ℓ have opposite-charge as expected for semileptonic B decay. The shaded histograms are the data for the case that the D_s and ℓ have the same charge: no signal is evident. The superimposed curves are a combined fit for the signal (Gaussian) and background (polynomial). A signal for $D^- \to \phi\pi^-$ is included in the curve superimposed in the upper-left-hand distribution.

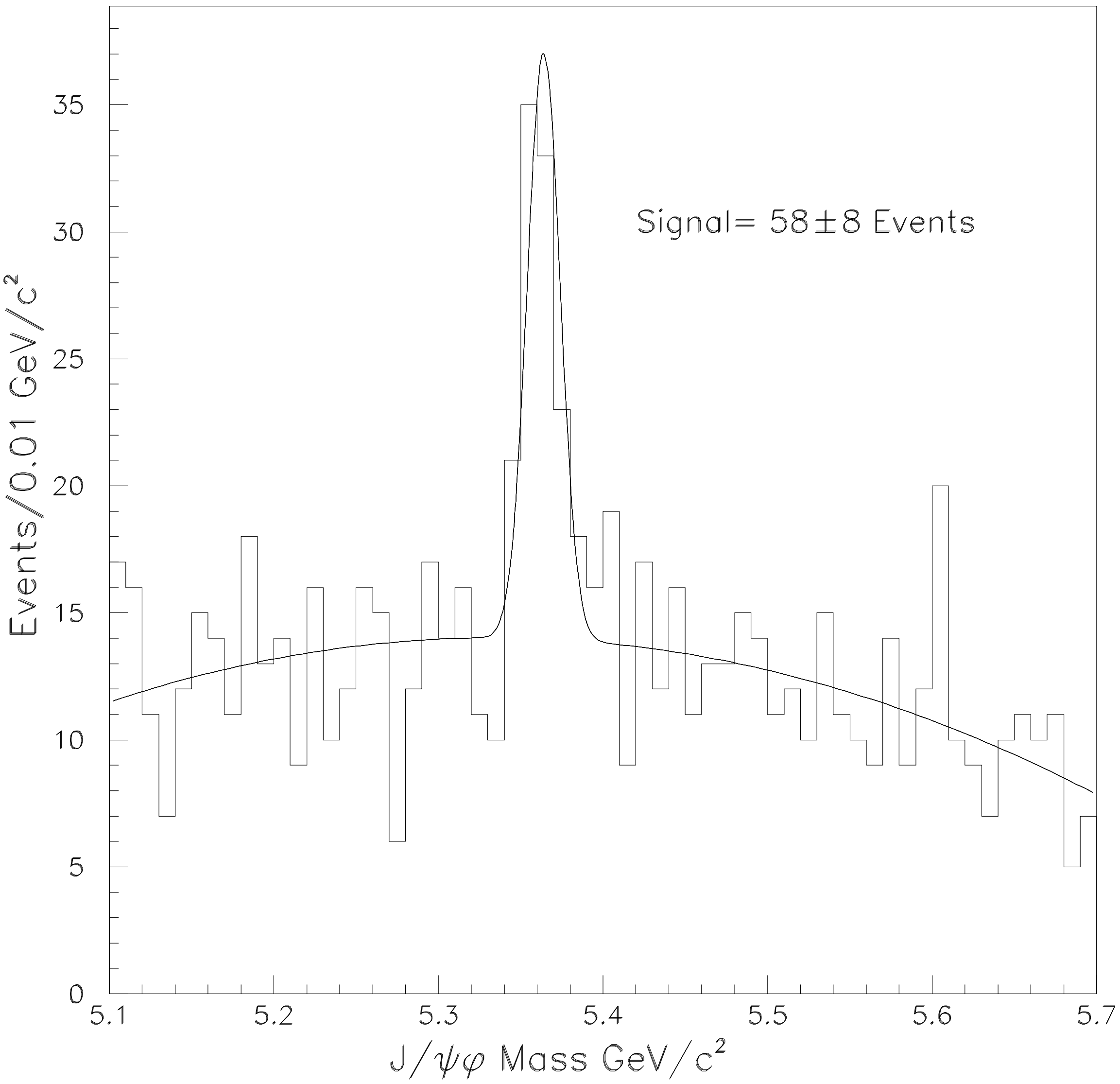

Figure 2: The mass spectrum of $B_s^0/\bar{B}_s^0 \to J/\psi\phi$ candidates used in the measurement of the B_s^0 lifetime. The curve is a fit of the data to a Gaussian for the signal plus a second order polynomial for the background.

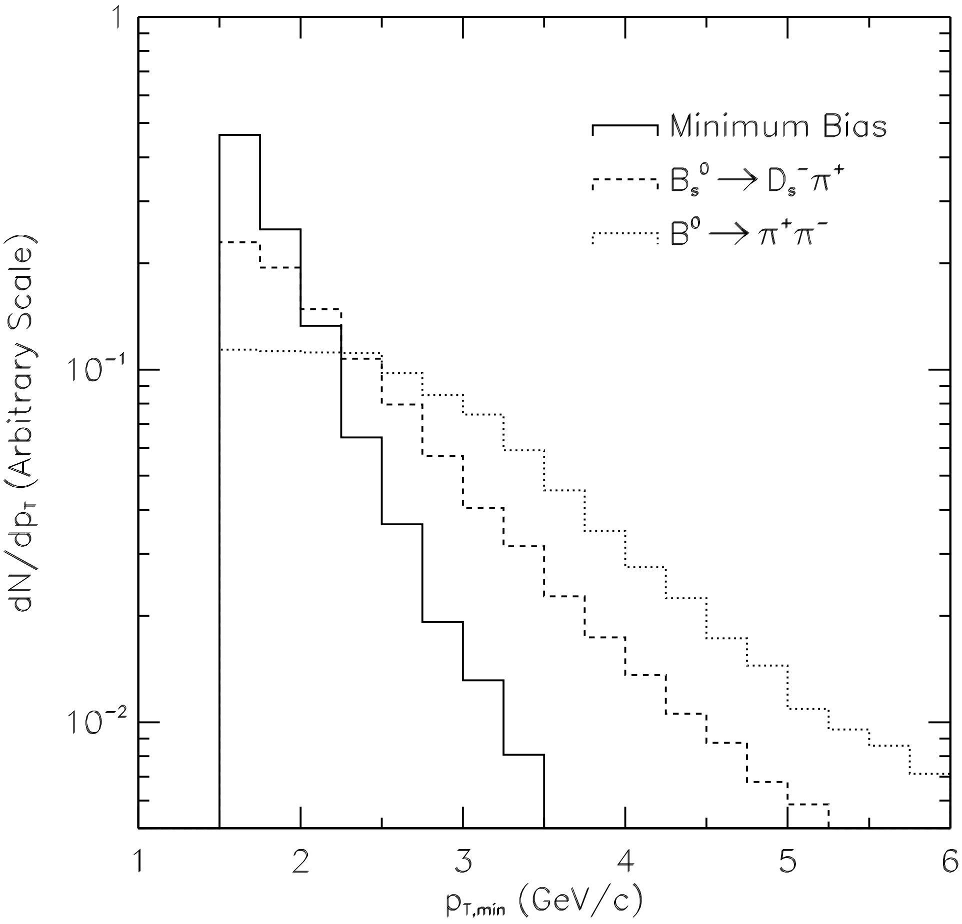

Figure 3: Distribution of the lower-p_T value for opposite charge track pairs with $\delta\phi_6 < 135°$ for CDF minimum bias data and the $B_s^0 \to D_s^- \pi^+$ and $B^0 \to \pi^+\pi^-$ decay channels.

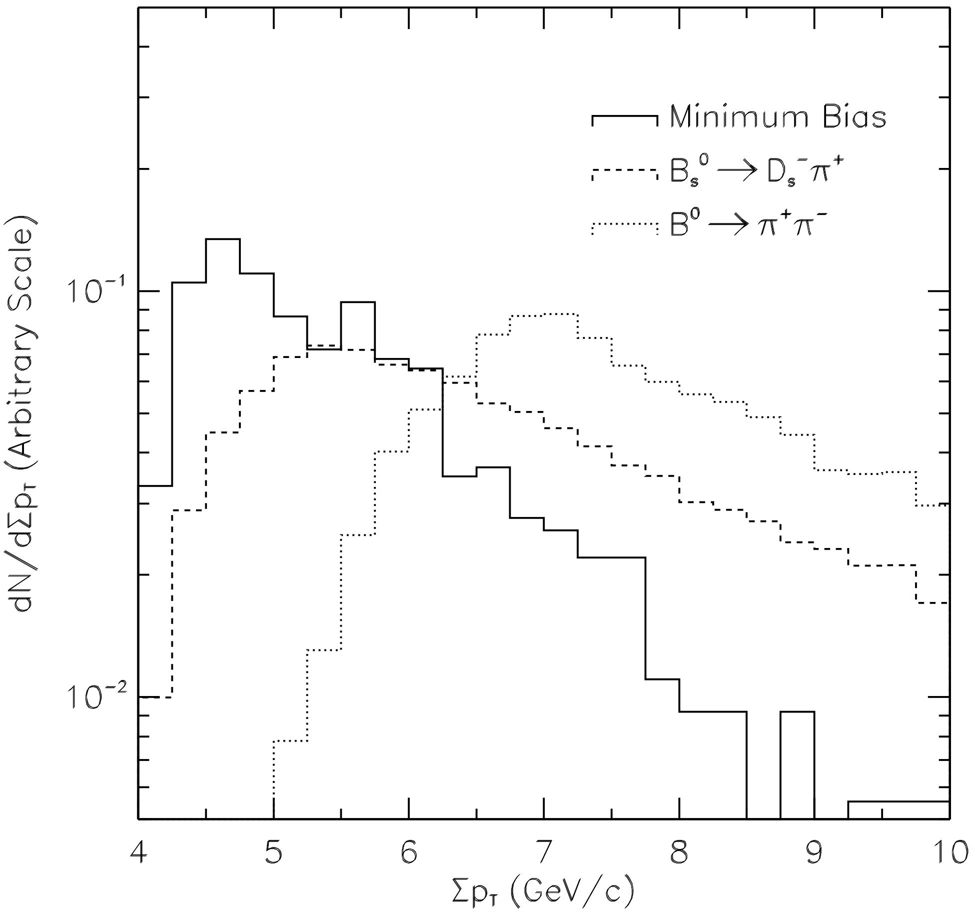

Figure 4: Distribution of Σp_T for opposite charge track pairs with $p_T > 2\,\mathrm{GeV}/c$ and $\delta\phi_6 < 135°$ for CDF minimum bias data and the $B_s^0 \rightarrow D_s^- \pi^+$ and $B^0 \rightarrow \pi^+\pi^-$ decay channels.

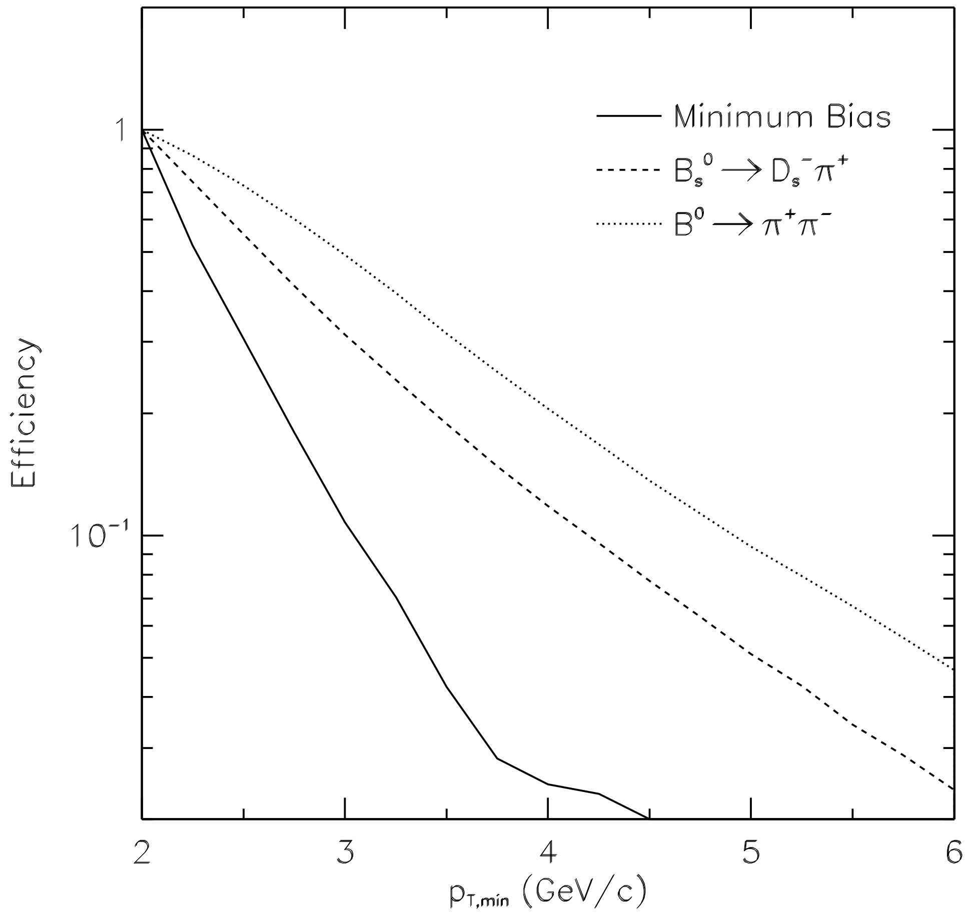

Figure 5: Relative efficiency of a requirement on the lower-p_T value for opposite charge track pairs with $\delta\phi_6 < 135°$ for CDF minimum bias data and the $B_s^0 \to D_s^- \pi^+$ and $B^0 \to \pi^+\pi^-$ decay channels compared to the nominal $p_{T,\min} = 2\,\mathrm{GeV}/c$.

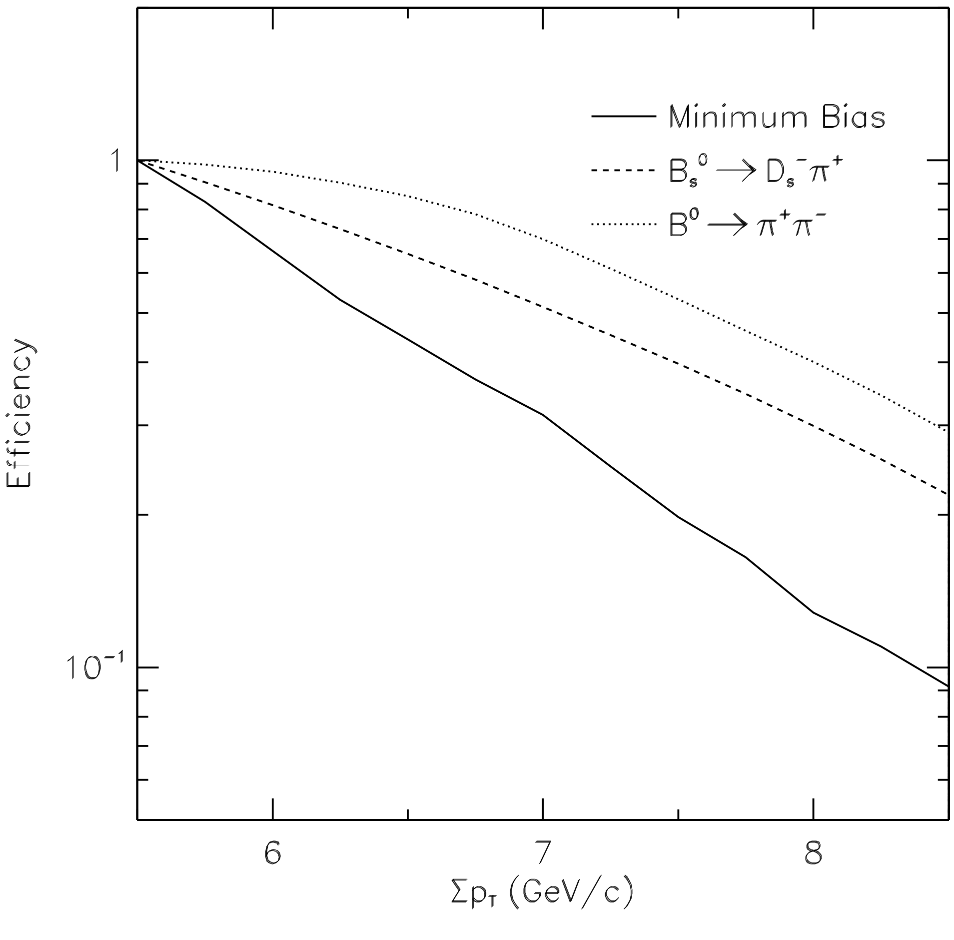

Figure 6: Relative efficiency of a requirement on Σp_T for opposite charge track pairs with $p_T > 2\,\mathrm{GeV}/c$ and $\delta\phi_6 < 135^\circ$ for CDF minimum bias data and the $B_s^0 \to D_s^- \pi^+$ and $B^0 \to \pi^+\pi^-$ decay channels compared to the nominal $(\Sigma p_T)_{\min} = 5.5\,\mathrm{GeV}/c$.

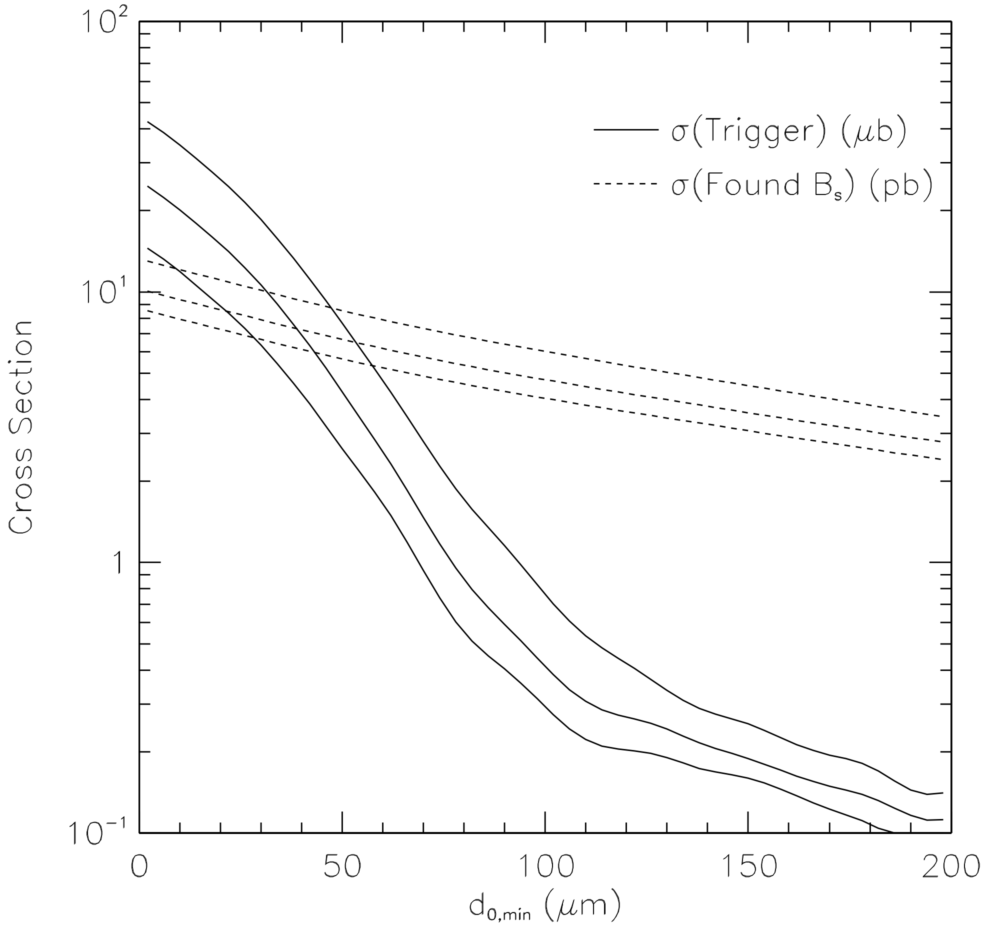

Figure 7: The dependence of the Level 2 cross section for the B_s selection as a function of the impact parameter selection requirement on both tracks from SVT simulations and the cross section for $B_s^0 \to D_s^- \pi^+$ events in the CDF reconstruction fiducial region. The three curves correspond to trigger scenarios A (upper), B (middle), and C (lower). The units for the Level 2 cross-section curve are microbarns, while the units for the $B_s^0 \to D_s^- \pi^+$ signal curves are picobarns.

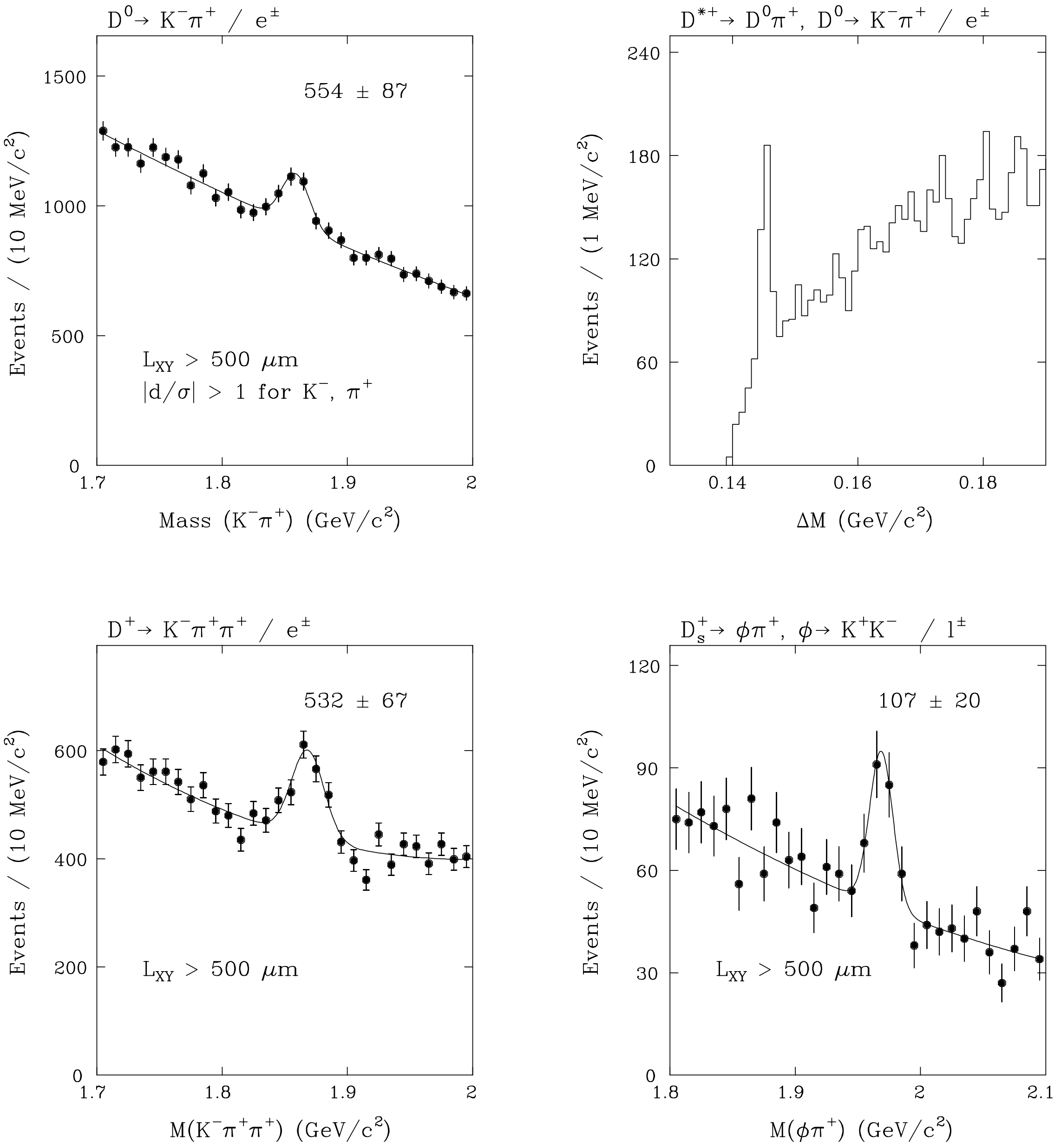

Figure 8: The mass spectra of D mesons reconstructed in inclusive lepton triggers: (a) upper-left: $D^0 \to K^-\pi^+$ (e trigger only); (b) upper-right: $D^{*+} \to D^0\pi^+$ (e trigger only), this is the mass difference $\Delta M = M(D^0\pi^+) - M(D^0)$; (c) lower-left: $D^+ \to K^-\pi^+\pi^+$ (e trigger only); and (d) lower-right: $D_s^+ \to \phi\pi^+$, with $\phi \to K^+K^-$ (e and μ trigger combined). The superimposed curves are a combined fit for the signal (Gaussian) and background (polynomial).

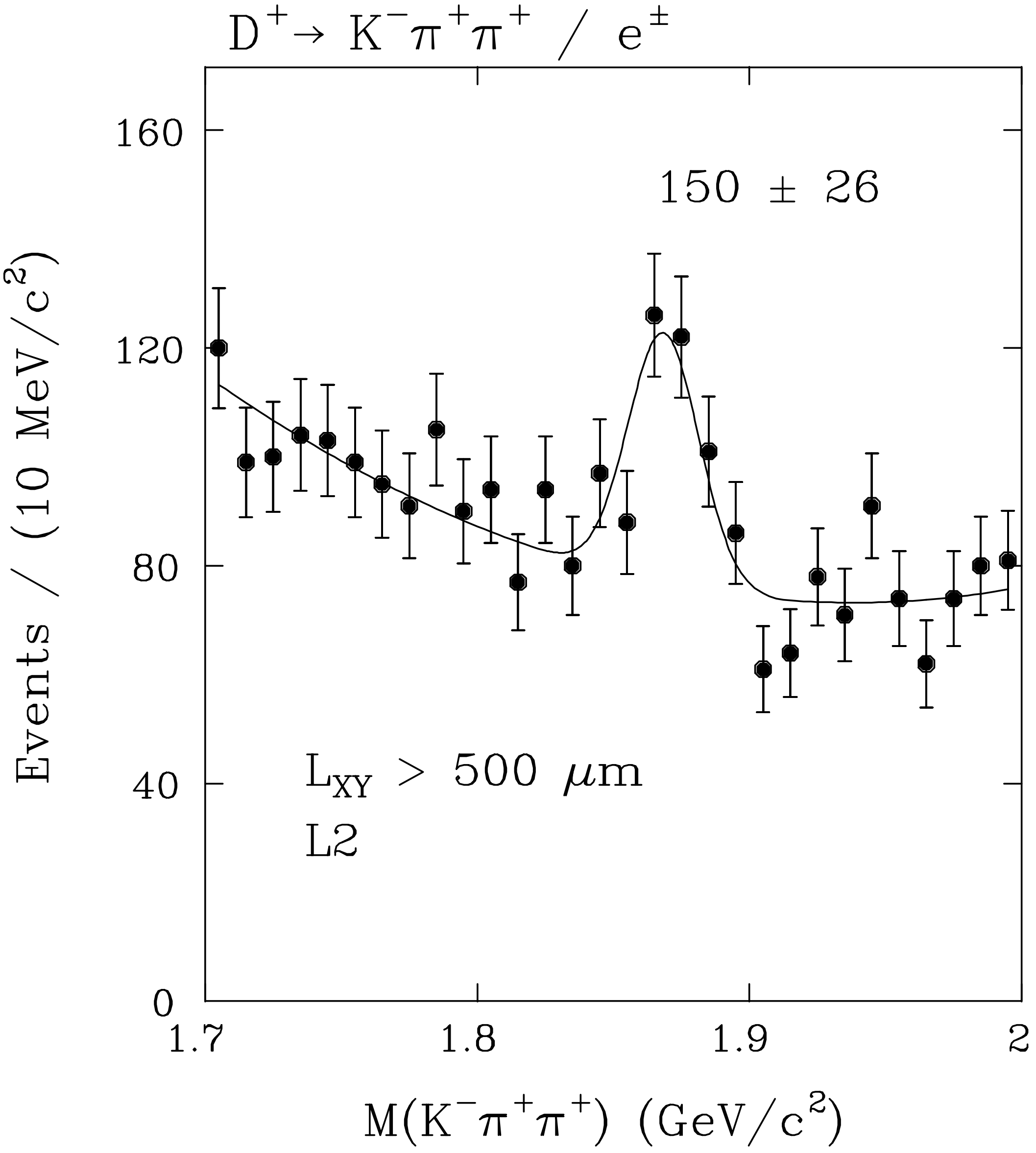

Figure 9: $D^+ \rightarrow K^-\pi^+\pi^+$ (e trigger only) after applying the Level 1 and Level 2 trigger selections to the event The superimposed curve is a combined fit for the signal (Gaussian) and background (polynomial).

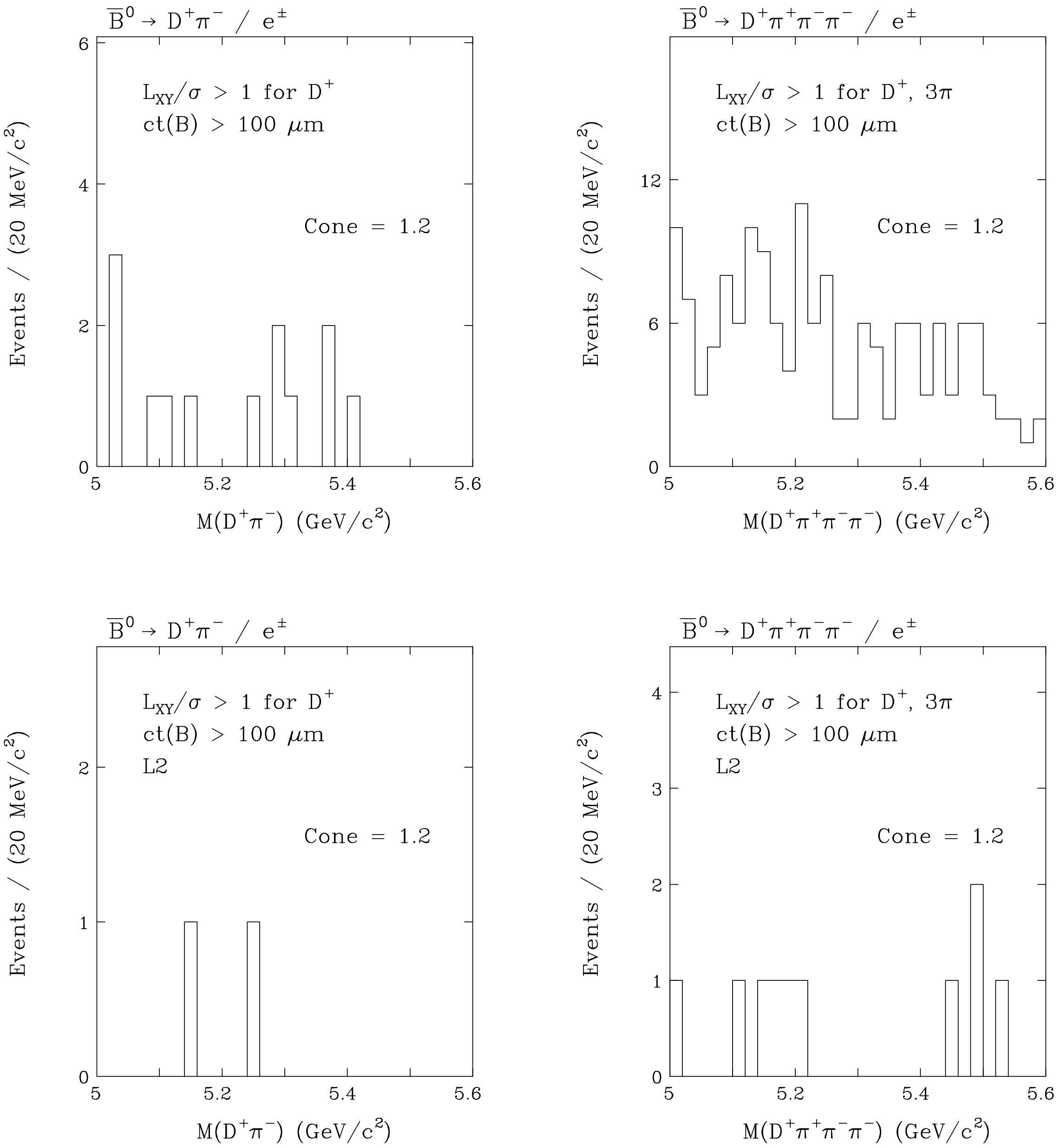

Figure 10: The mass distributions when a D^+ candidate is combined with one track (π^-) or three tracks ($\pi^+\pi^-\pi^-$). (a) upper-left: the $D^+\pi^-$ mass distribution when no trigger requirements are imposed on the event; (b) upper-right: the $D^+\pi^+\pi^-\pi^-$ mass distribution when no trigger requirements are imposed on the event; (c) lower-left: the $D^+\pi^-$ mass distribution when the Level 1 and Level 2 trigger requirements are imposed on the event; (d) lower-right: the $D^+\pi^+\pi^-\pi^-$ mass distribution when the Level 1 and Level 2 trigger requirements are imposed on the event. The bin size is 20 MeV/c^2, and there are thirty bins total in each distribution. Our expected B mass resolution is approximately 10 MeV/c^2.

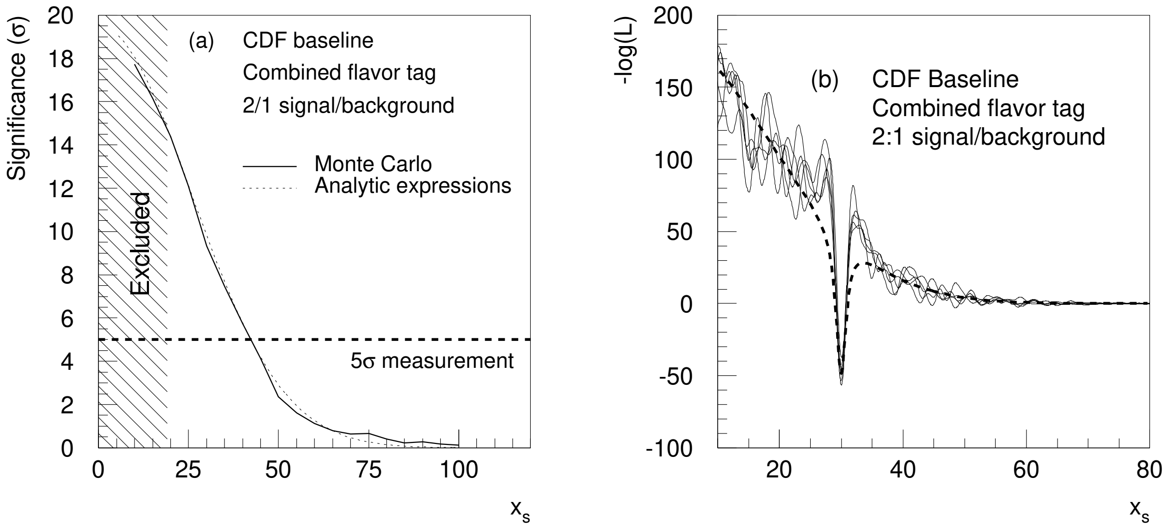

Figure 11: (a) A comparison of the expected significance of a measurement x_s determined using analytic and Monte Carlo calculations. (b) A comparison of the shapes of the $-\log\mathcal{L}$ curves from several simulated experiments with $x_s = 30$ (solid curves) and an analytic expression (dashed curve).

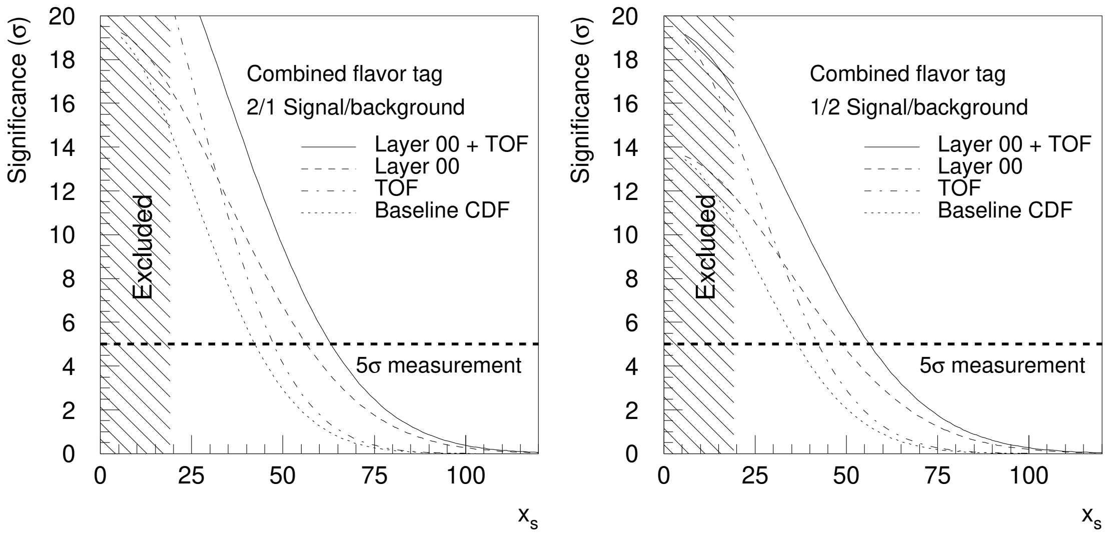

Figure 12: Effects of background levels on x_s reach in Run II for the CDF baseline configuration and with the beyond the baseline upgrades assuming $N(B_s^0) = 20,000$ and signal-to-background ratios of 2:1 (a) and 1:2 (b).

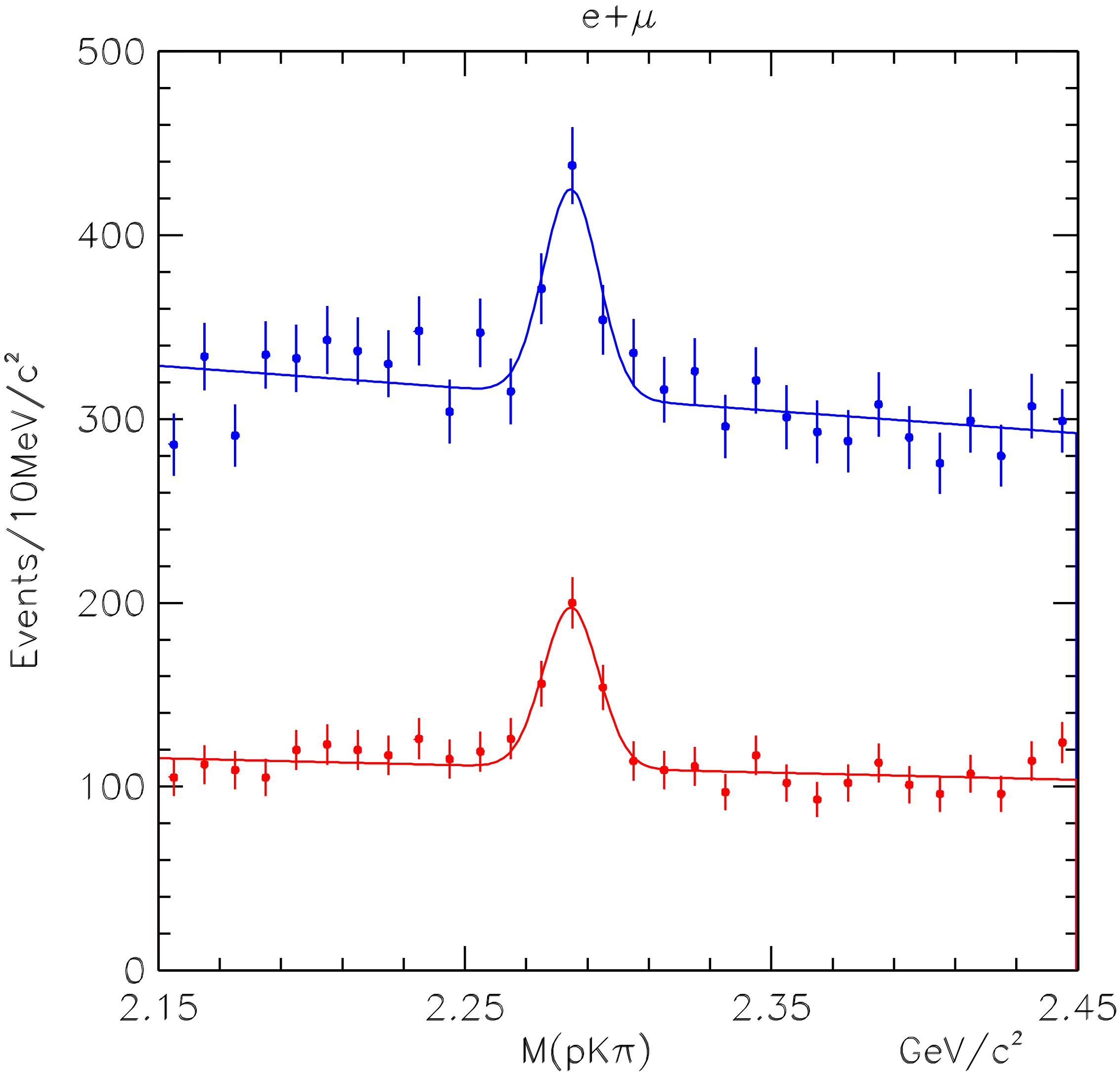

Figure 13: The improvement in signal to background in the signature $\Lambda_c^+ \to pK^-\pi^+$ when the proton is identified using dE/dx in the CTC. The curves are fits to the data with a Gaussian for the signal and a linear background. The upper curve shows the signal before proton identification, and the lower curve shows the signal after proton identification.

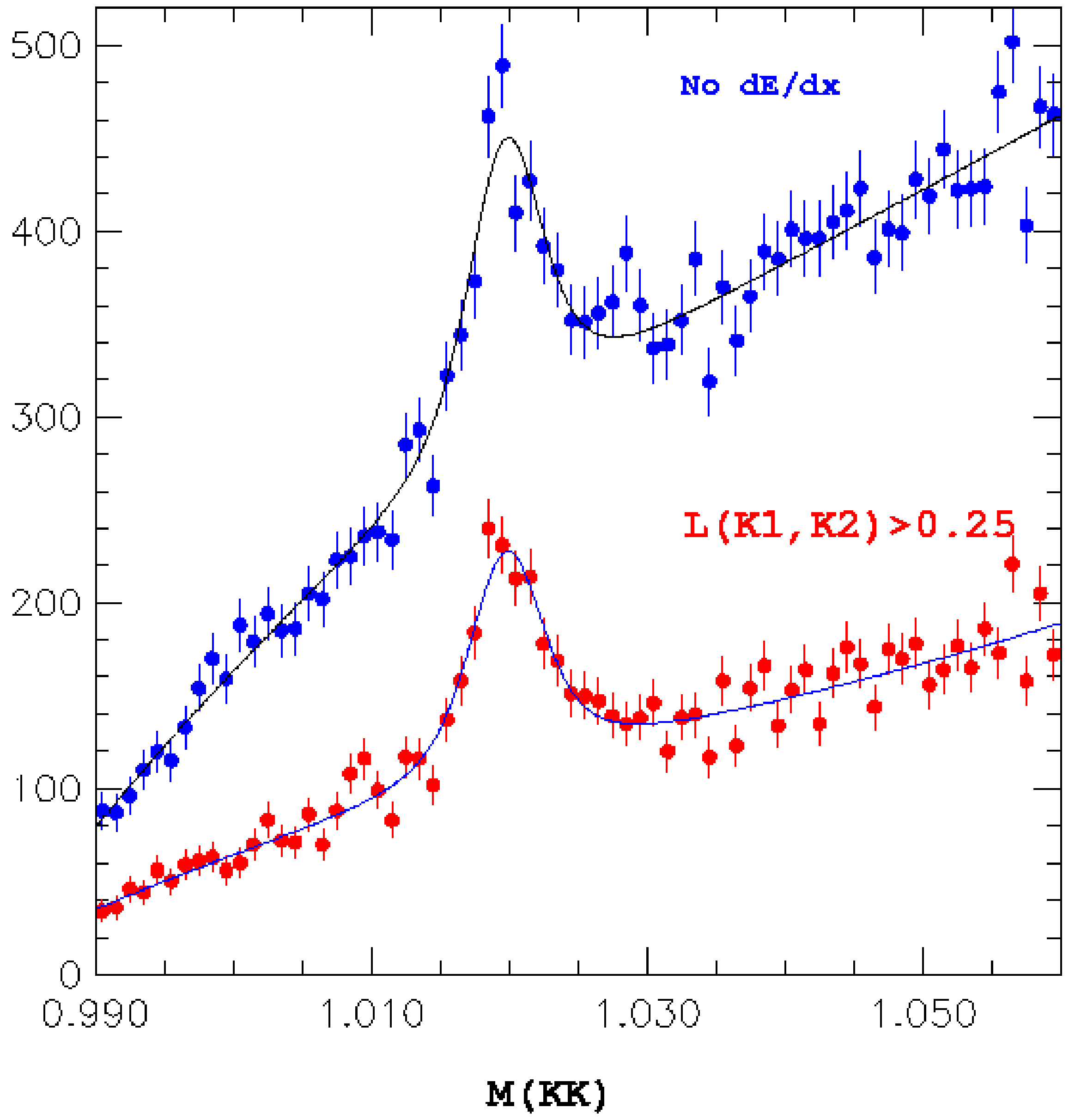

Figure 14: The improvement in signal to background in the signature $\phi \to K^+K^-$ when the kaons are identified using dE/dx in the CTC. These ϕ are from semileptonic B decay. The curves are fits to the data with a Gaussian for the signal and a polynomial to describe the background. The upper curve shows the signal before kaon identification, and the lower curve shows the signal after kaon identification.